

SHARP INEQUALITIES INVOLVING THE CHEEGER CONSTANT OF PLANAR CONVEX SETS

ILIAS FTOUHI, ALBA LIA MASIELLO, GLORIA PAOLI

ABSTRACT. We are interested in finding sharp bounds for the Cheeger constant h via different geometrical quantities, namely the area $|\cdot|$, the perimeter P , the inradius r , the circumradius R , the minimal width ω and the diameter d . We provide new sharp inequalities between these quantities for planar convex bodies and enounce new conjectures based on numerical simulations. In particular, we completely solve the Blaschke–Santaló diagrams describing all the possible inequalities involving the triplets (P, h, r) , (d, h, r) and (R, h, r) and describe some parts of the boundaries of the diagrams of the triplets (ω, h, d) , (ω, h, R) , (ω, h, P) , $(\omega, h, |\cdot|)$, (R, h, d) and (ω, h, r) .

KEYWORDS: Cheeger constant, convex sets, Blaschke–Santaló diagrams, sharp inequalities.
MSC 2020: 52A10, 52A40, 65K15.

1. INTRODUCTION

Let Ω be a bounded subset of \mathbb{R}^2 . The Cheeger constant of Ω , introduced in and by Jeff Cheeger in [12] in connection with the first eigenvalue of the Laplacian, is defined as

$$(1) \quad h(\Omega) := \inf \left\{ \frac{P(E)}{|E|} : E \text{ measurable, } E \subseteq \Omega, |E| > 0 \right\},$$

where $P(E)$ is the perimeter of E in the sense of De Giorgi and $|E|$ is the area of E . The minimum in (1) is achieved when Ω has Lipschitz boundary, see as a reference [32], and the set E that realizes this minimum is called a *Cheeger set* of Ω . For the properties of the Cheeger constant and for an introductory survey, see for example [1, 27, 32]. In particular, in the case of convex sets, the authors in [1] prove that the Cheeger set is unique and, in this case, we will denote it by C_Ω . At last, a complete characterization of the Cheeger sets of planar convex bodies is provided in [27].

The problem of finding the Cheeger constant of a domain has been widely considered and has several applications (see [32] for a general overview). One of the possible interpretations of the Cheeger constant can be found for instance in the context of maximal flow and minimal cut problems (see [40]) which has applications in medical images processing (see [4]). The Cheeger problem appears also in the study of plate failure under stress (see [28]). It is then useful to have estimates of the Cheeger constant in terms of geometric quantities that can be easily computed.

In the present paper, we are interested in describing all the possible inequalities involving the Cheeger constant of a given compact and convex set $\Omega \subset \mathbb{R}^2$ with nonempty interior and the following geometrical quantities: the area $|\Omega|$, the perimeter $P(\Omega)$, the inradius $r(\Omega)$, the circumradius $R(\Omega)$, the minimal width $\omega(\Omega)$ and the diameter $d(\Omega)$. We are then aiming to study the Blaschke–Santaló diagrams involving those functionals and collect them all in one single paper together with new conjectures.

A Blaschke–Santaló diagram is a tool that allows to visualize all the possible inequalities between three geometric quantities. More precisely, we consider three homogeneous shape functionals (J_1, J_2, J_3) , that is to

say that for every $i \in \{1, 2, 3\}$ there exists $\alpha_i \in \mathbb{R}$ such that $J_i(t\Omega) = t^{\alpha_i} J_i(\Omega)$ for every $t > 0$, and we want to find a system of inequalities describing the set

$$\{(J_1(\Omega), J_2(\Omega)) \mid J_3(\Omega) = 1, \Omega \in \mathcal{K}^2\},$$

where we denote by \mathcal{K}^2 the class of planar, compact and convex sets with nonempty interior.

This kind of diagram was introduced by Blaschke in [5], in order to investigate all the possible relations between the volume, the surface area and the integral mean curvature in the class of compact convex sets in \mathbb{R}^3 . Following the idea of Blaschke, Santaló in [36] proposed the study of these diagrams for all the triplets of the following geometrical quantities: area, perimeter, inradius, circumradius, minimal width and diameter. These diagrams were studied for the class of convex sets and six of them are still not completely solved. We refer to the introduction in [13] for an accurate and updated state of art. Moreover, for classical results about Blaschke–Santaló diagrams, we refer for example to [9, 21, 22, 24, 25, 23, 36] and for more recent results, we provide the following non-exhaustive list of works [10, 11, 13, 15, 17, 18, 31].

In [14] and [16] the author studies Blaschke–Santaló diagram involving the Cheeger constant. More precisely, in [14], it the Blaschke–Santaló diagram involving the Cheeger constant, the area and the inradius is fully characterized. It is proved that, if $\Omega \in \mathcal{K}^2$, then

$$(2) \quad \frac{1}{r(\Omega)} + \frac{\pi r(\Omega)}{|\Omega|} \leq h(\Omega) \leq \frac{1}{r(\Omega)} + \sqrt{\frac{\pi}{|\Omega|}},$$

where the upper bound in (2) is achieved by (and only by) sets that are homothetic to their form bodies (see Definition 2.10), for instance, sets that are homothetic to their form bodies, meanwhile the lower one is achieved by (and only by) stadiums. On the other hand, in [16], the diagram involving the Cheeger constant, the area and the perimeter is fully characterized and it is proved that if $\Omega \in \mathcal{K}^2$, then

$$(3) \quad \frac{P(\Omega) + \sqrt{4\pi|\Omega|}}{2|\Omega|} \leq h(\Omega) \leq \frac{P(\Omega)}{|\Omega|},$$

where the upper bound is achieved by any set that is Cheeger of itself (in particular stadiums), meanwhile the lower one is achieved, for example, by circumscribed polygons.

Now, let us state the main results of the paper. In order to do so, we need to define the following classes of admissible sets (we refer to [38, Table 2.1] for the associated constraints):

- (1) $\mathcal{K}_{P,r}^2 = \{\Omega \in \mathcal{K}^2 : P(\Omega) = P, r(\Omega) = r\}$, where $P \geq 2\pi r$;
- (2) $\mathcal{K}_{d,r}^2 = \{\Omega \in \mathcal{K}^2 : d(\Omega) = d, r(\Omega) = r\}$, where $d \geq 2r$;
- (3) $\mathcal{K}_{R,r}^2 = \{\Omega \in \mathcal{K}^2 : R(\Omega) = R, r(\Omega) = r\}$, where $R \geq r$;
- (4) $\mathcal{K}_{\omega,d}^2 = \{\Omega \in \mathcal{K}^2 : \omega(\Omega) = \omega, d(\Omega) = d\}$, where $\omega \leq d$;
- (5) $\mathcal{K}_{\omega,R}^2 = \{\Omega \in \mathcal{K}^2 : \omega(\Omega) = \omega, R(\Omega) = R\}$, where $2R \geq \omega$;
- (6) $\mathcal{K}_{\omega,P}^2 = \{\Omega \in \mathcal{K}^2 : \omega(\Omega) = \omega, P(\Omega) = P\}$, where $P \geq \pi\omega$;
- (7) $\mathcal{K}_{\omega,A}^2 = \{\Omega \in \mathcal{K}^2 : \omega(\Omega) = \omega, |\Omega| = A\}$, where $\sqrt{3}A \geq \omega^2$;
- (8) $\mathcal{K}_{R,d}^2 = \{\Omega \in \mathcal{K}^2 : R(\Omega) = R, d(\Omega) = d\}$, where $\sqrt{3}R \leq d < 2R$;
- (9) $\mathcal{K}_{\omega,r}^2 = \{\Omega \in \mathcal{K}^2 : \omega(\Omega) = \omega, r(\Omega) = r\}$, where $2r < \omega \leq 3r$;
- (10) $\mathcal{K}_{R,A}^2 = \{\Omega \in \mathcal{K}^2 : R(\Omega) = R, |\Omega| = A\}$, where $A \leq \pi R^2$;
- (11) $\mathcal{K}_{P,R}^2 = \{\Omega \in \mathcal{K}^2 : P(\Omega) = P, R(\Omega) = R\}$, where $4R < P \leq 2\pi R$;

$$(12) \mathcal{K}_{P,d}^2 = \{\Omega \in \mathcal{K}^2 : P(\Omega) = P, d(\Omega) = d\}, \text{ where } 2d < P \leq \pi d;$$

$$(13) \mathcal{K}_{d,A}^2 = \{\Omega \in \mathcal{K}^2 : d(\Omega) = d, |\Omega| = A\}, \text{ where } \pi d^2 \geq 4A.$$

Firstly, let us state the following existence result.

Theorem 1.1. *Let $\Omega \in \mathcal{K}^2$, then the minimization and the maximization shape optimization problems of the Cheeger constant $h(\Omega)$ admit a solution in the classes of sets defined in (1) – (13).*

In the following theorem, we consider the triplets of functionals for which we are able to provide the complete description of the related Blaschke–Santaló diagrams. For the precise definitions of the below-mentioned extremal sets, see Section 2.2 and for the explicit bounds, see Propositions 4.1, 4.2 and 4.5. At last, for the description of the corresponding diagrams we refer to Proposition 4.7.

Theorem 1.2. *The following results hold*

- (i) *The maximum and the minimum of the Cheeger constant in $\mathcal{K}_{P,r}^2$ are respectively achieved by sets that are homothetic to their form bodies and by stadiums.*
- (ii) *The maximum of the Cheeger constant in $\mathcal{K}_{d,r}^2$ is achieved by symmetrical two-cup bodies. On the other hand, there exists $D_0 > 0$ such that if $d \geq rD_0$, then the minimum of the Cheeger constant in $\mathcal{K}_{d,r}^2$ is achieved by symmetrical spherical slices, while, if $d < rD_0$, the minimum is achieved by regular smoothed nonagons.*
- (iii) *The maximum and the minimum of the Cheeger constant in $\mathcal{K}_{R,r}^2$ are respectively achieved by symmetrical two-cup bodies and symmetrical spherical slices.*

As far as the classes of sets $\mathcal{K}_{\omega,d}^2$, $\mathcal{K}_{R,\omega}^2$, $\mathcal{K}_{\omega,P}^2$ and $\mathcal{K}_{A,\omega}^2$ are concerned, we are able to identify parts of the boundary of the corresponding Blaschke–Santaló diagrams, see Propositions 5.1, 5.3, 5.7 and 5.5 for the explicit bounds. For the class $\mathcal{K}_{d,R}^2$, we are able to solve the maximization problem, see Proposition 5.8, meanwhile, for the class $\mathcal{K}_{\omega,r}^2$ we are able to solve the minimization one, see Proposition 5.9. Throughout the paper, different strategies of proofs are used to obtain all the aforementioned results.

As far as the classes $\mathcal{K}_{A,R}^2$, $\mathcal{K}_{R,P}^2$, $\mathcal{K}_{P,d}^2$ and $\mathcal{K}_{A,d}^2$ are concerned, we are not able to identify any parts of the boundaries of the corresponding Blaschke–Santaló diagrams. Nevertheless, in the appendix we present the best bounds that we managed to obtain by combining the known inequalities involving those functionals.

The paper is organized as follows: in Section 2, we state the preliminary results, the definitions used throughout the paper and the known inequalities relating the Cheeger constant to one of the geometric quantities taken into consideration. Section 3 is dedicated to the description of the numerical methods used to compute the functionals and to approximate the Blaschke–Santaló diagrams. In Section 4, we prove the main results, that are Theorem 1.1 and Theorem 1.2. Section 5 is dedicated to the results that we have obtained for the classes of sets $\mathcal{K}_{\omega,d}^2$, $\mathcal{K}_{R,\omega}^2$, $\mathcal{K}_{\omega,P}^2$, $\mathcal{K}_{A,\omega}^2$, $\mathcal{K}_{d,R}^2$ and $\mathcal{K}_{\omega,r}^2$. Finally, in Section 6, we state some relevant conjectures and collect all the inequalities proved in the paper in the Appendix.

2. NOTATIONS AND PRELIMINARIES

Throughout this article, $\|\cdot\|$ will denote the Euclidean norm in \mathbb{R}^2 , while (\cdot) is the standard Euclidean scalar product in \mathbb{R}^2 . We denote by $P(\Omega)$ the perimeter of Ω and by $|\Omega|$ the volume of Ω . Moreover, B_r is the closed ball of radius $r > 0$ centered at the origin, while \mathbb{S}^1 is the unit sphere in \mathbb{R}^2 . In the following, we work with the class of sets \mathcal{K}^2 , defined as

$$\mathcal{K}^2 := \{\Omega \mid \Omega \text{ is a compact, bounded and convex set with nonempty interior of } \mathbb{R}^2\} \setminus \{\emptyset\}.$$

2.1. Classical results and preliminary lemmas. We provide the classical definitions and results that we need in the following.

Definition 2.1. Let $\Omega, K \subset \mathbb{R}^2$ two convex bounded sets. We define the Minkowski sum (+) and difference (\sim) as

$$\begin{aligned}\Omega + K &:= \{x + y : x \in \Omega, y \in K\}, \\ \Omega \sim K &:= \{x \in \mathbb{R}^2 : x + K \subseteq \Omega\}.\end{aligned}$$

We now recall the definition of the Hausdorff distance.

Definition 2.2. Let $\Omega, K \subset \mathbb{R}^2$ be two non-empty compact sets, we define the Hausdorff distance between Ω and K as follows:

$$d_{\mathcal{H}}(\Omega, K) := \inf \{ \varepsilon > 0 : \Omega \subset K + B_{\varepsilon}, K \subset \Omega + B_{\varepsilon} \},$$

where B_{ε} is the ball of radius ε centered in the origin.

Let $\{\Omega_k\}_{k \in \mathbb{N}}$ be a sequence of non-empty, compact, bounded convex subsets of \mathbb{R}^2 , we say that Ω_k converges to Ω in the Hausdorff sense and we denote

$$\Omega_k \xrightarrow{\mathcal{H}} \Omega,$$

if and only if $d_{\mathcal{H}}(\Omega_k, \Omega) \rightarrow 0$ as $k \rightarrow \infty$.

We recall that by Blaschke's selection Theorem (see for example [37, Theorem 1.8.7]), every bounded sequence of nonempty compact convex sets has a subsequence that converges in the Hausdorff sense to a convex set.

Let us now recall the following definitions:

Definition 2.3. Let $\Omega \in \mathcal{K}^2$. The distance function from the boundary of Ω is the function $\text{dist}(\cdot, \partial\Omega) : \Omega \rightarrow [0, +\infty[$ defined as

$$\text{dist}(x, \partial\Omega) = \inf_{y \in \partial\Omega} \|x - y\|.$$

The inradius of Ω is defined as

$$r(\Omega) := \sup_{x \in \Omega} \text{dist}(x, \partial\Omega),$$

and the circumradius of Ω is defined as

$$R(\Omega) := \min_{x \in \Omega} \max_{y \in \partial\Omega} \|x - y\|.$$

Let us now introduce the support function of a convex set:

Definition 2.4. Let $\Omega \in \mathcal{K}^2$. The support function of Ω is defined as

$$p_{\Omega}(y) := \max_{x \in \Omega} (x \cdot y), \quad y \in \mathbb{R}^2.$$

In this paper, we will also consider the minimal width (or thickness) of a convex set, that is to say the minimal distance between two parallel supporting hyperplanes. More precisely, we have

Definition 2.5. Let $\Omega \in \mathcal{K}^2$. The width of Ω in the direction $y \in \mathbb{S}^1$ is defined as

$$\omega_{\Omega}(y) := p_{\Omega}(y) + p_{\Omega}(-y)$$

and the minimal width of Ω as

$$\omega(\Omega) := \min\{\omega_{\Omega}(y) \mid y \in \mathbb{S}^1\}.$$

We introduce the inner parallel set of a convex set Ω .

Definition 2.6. Let Ω be a bounded and convex set. The inner parallel set of Ω at distance $t \in [0, r(\Omega)]$ is

$$\Omega_{-t} := \{x \in \Omega : \text{dist}(x, \partial\Omega) \geq t\}.$$

Remark 2.7. We remark that, by Definition 2.6, we have

$$\Omega_{-t} = \Omega \sim tB_1.$$

Moreover, we observe that for any $y \in \mathbb{S}^1$ and for every $\Omega, K \in \mathcal{K}^2$, one has

$$p_{\Omega \sim K}(y) \leq p_\Omega(y) - p_K(y),$$

see e.g. [37, Section 3.1, page 148].

Therefore, in the case $K = tB_1$, this reads

$$(4) \quad p_{\Omega_{-t}}(y) \leq p_\Omega(y) - t.$$

Moreover, as it is observed in [26, Proposition 3.2], one has

$$(5) \quad R(\Omega + K) \leq R(\Omega) + R(K)$$

with equality if $K = tB_1$.

We are now in position to prove the following lemma:

Lemma 2.8. Let $\Omega \in \mathcal{K}^2$. We have for every $t \in [0, r(\Omega)]$:

$$(6) \quad r(\Omega_{-t}) = r(\Omega) - t,$$

$$(7) \quad d(\Omega_{-t}) \leq d(\Omega) - 2t,$$

$$(8) \quad \omega(\Omega_{-t}) \leq \omega(\Omega) - 2t,$$

$$(9) \quad R(\Omega_{-t}) \leq R(\Omega) - t,$$

$$(10) \quad P(\Omega_{-t}) \leq P(\Omega) - 2\pi t.$$

Proof. • The proof of (6) can be found in [30, Lemma 1.4].

- Let us now prove (7). Let $x_t, y_t \in \Omega_{-t}$ be two diametrical points of Ω_{-t} (i.e., such that $\|x_t - y_t\| = d(\Omega_{-t})$). We denote by $x, y \in \Omega$ the points corresponding to the intersection of the line containing x_t and y_t with the boundary of Ω . We have

$$d(\Omega) \geq \|x - y\| = \|x - x_t\| + \|x_t - y_t\| + \|y_t - y\| = \|x - x_t\| + d(\Omega_{-t}) + \|y_t - y\| \geq d(\Omega_{-t}) + 2t,$$

where the last inequality is a consequence of the fact that $x_t, y_t \in \Omega_{-t} = \{x \in \Omega \mid \text{dist}(x, \partial\Omega) \geq t\}$.

- The proof of (8) follows directly from the definition of the minimal width (Definition 2.5) and (4).
- We prove now (9). As observed in Remark 2.7, and, in particular, by formula (5), for every $\Omega \in \mathcal{K}^2$, we have that $R(\Omega + tB_1) = R(\Omega) + t$. Thus, we have

$$R(\Omega_{-t}) = R(\Omega_{-t} + tB_1) - t \leq R(\Omega) - t.$$

The last inequality follows from the inclusion $\Omega_{-t} + tB_1 \subset \Omega$ and the monotonicity of the circumradius with respect to inclusions.

- Formula (10) can be obtained as a consequence of the classical Steiner formula

$$P(K + tB_1) = P(K) + 2\pi t,$$

see for example [37, Section 4.1], and the fact that the perimeter is monotone with respect to the inclusion for convex sets. Indeed, since $\Omega_{-t} + tB_1 \subset \Omega$, we have $P(\Omega_{-t} + tB_1) \leq P(\Omega)$, which is equivalent by the Steiner formula to $P(\Omega_{-t}) + 2\pi t \leq P(\Omega)$.

□

The following Lemma will play a key role in the proof of Theorem 1.2.

Lemma 2.9. *Let $\Omega \in \mathcal{K}^2$. We assume that there exists a continuous function $g^\Omega : [0, r(\Omega)] \rightarrow \mathbb{R}$ such that*

$$(11) \quad \forall t \in [0, r(\Omega)], \quad |\Omega_{-t}| \leq g^\Omega(t), \quad (\text{resp. } |\Omega_{-t}| \geq g^\Omega(t)),$$

and that

$$(12) \quad G_\Omega := \{ t \in [0, r(\Omega)] : g^\Omega(t) = \pi t^2 \} \neq \emptyset.$$

We have

$$(13) \quad h(\Omega) \geq \frac{1}{t_{g^\Omega}} \quad (\text{resp. } h(\Omega) \leq \frac{1}{t_{g^\Omega}}),$$

where t_{g^Ω} is the smallest (resp. largest) solution to the equation $g^\Omega(t) = \pi t^2$ on $[0, r(\Omega)]$.

Proof. From [27, Theorem 1], we know that there exists a unique $t = t_\Omega > 0$ such that $|\Omega_{-t}| = \pi t^2$ and $h(\Omega) = 1/t_\Omega$. It is then clear that, if there exists a function $g(t)$ such that (11) and (12) hold, then, the smallest (resp. largest) element $t_{g^\Omega} \in G_\Omega$ must satisfy (13) (see Figure 1). \square

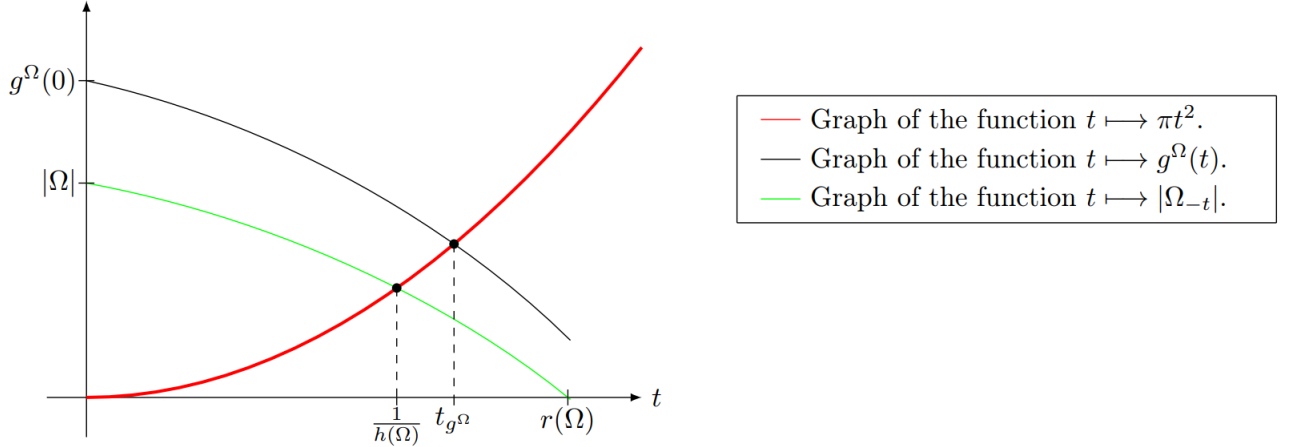


FIGURE 1. The idea of the proof of Lemma 2.9.

2.2. Extremal sets and their properties. In this Section, we describe special planar shapes that appear in the statement of the main results.

Firstly, let us recall the definition of the form body of a convex set Ω , following [37]: a point $x \in \partial\Omega$ is called *regular* if the supporting hyperplane at x is uniquely defined. The set of all regular points of $\partial\Omega$ is denoted by $\text{reg}(\Omega)$. We also let $U(\Omega)$ denote the set of all outward pointing unit normals to $\partial\Omega$ at points of $\text{reg}(\Omega)$.

Definition 2.10. *The form body Ω^* of a set $\Omega \in \mathcal{K}^2$ is defined as*

$$\Omega^* = \bigcap_{u \in U(\Omega)} \{x \in \mathbb{R}^2 : (x, u) \leq 1\}.$$

Convex sets that are homothetic to their form bodies will appear in the following as extremal sets. In particular, a polygon whose incircle touches all its sides is homothetic to its form body.

Definition 2.11. A stadium \mathcal{R} is defined as the convex hull of the union of two balls in \mathbb{R}^2 with the same radius, see Figure 2.



FIGURE 2. A stadium.

Definition 2.12. The symmetrical spherical slice \mathcal{S} of diameter d and width $\omega \leq d$ is the convex set obtained by the intersection of a ball of radius $d/2$ and a strip of width ω centered at the center of the ball, see Figure 3.

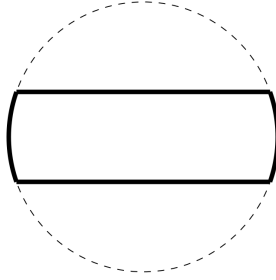


FIGURE 3. A symmetrical spherical slice.

Definition 2.13. A two-cup body \mathcal{C} is the convex hull of a ball in \mathbb{R}^2 with two points that are symmetric with respect to the center of the ball, see Figure 4. In particular, a two-cup body is homothetic to its form body.

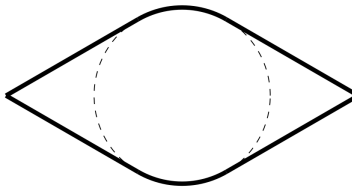


FIGURE 4. A two-cup body.

Definition 2.14. A subequilateral triangle T_I is an isosceles triangle with two equal angles greater than $\pi/3$.

The following class of sets (introduced in [43], see also [36]) represents a way to pass in a continuous manner with respect to the Hausdorff distance from the equilateral triangle to the Reuleaux triangle.

Definition 2.15. A Yamanouti set Y is the convex hull of an equilateral triangle and three circular arcs of equal radius, whose centers are each of the vertices of this triangle; the radius of these circular arcs is less than the length of the edge of the triangle, see Figure 5.

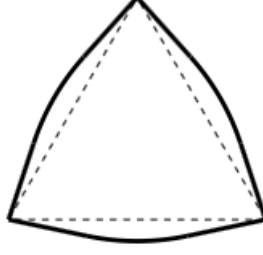


FIGURE 5. A Yamanouti set.

In [13], the authors define the smoothed regular nonagon as follows:

Definition 2.16. Let $r > 0$ and $2r < d < 2\sqrt{3}r$. The smoothed regular nonagon of inradius r and diameter d , that we denote by $\mathcal{N}_{r,d}$, is the convex set enclosed in an equilateral triangle T_E with barycenter in the origin and such that $r(T_E) = r$, obtained following the construction below. Let η_i the normal angles to the sides of T_E and let

$$\tau := (3 + \sqrt{d^2 - 3r^2})/2, \quad \text{and} \quad h := \sqrt{d^2 - \tau^2}.$$

We now define the points A_i, B_i, M_i , for $i = 1, 2, 3$:

$$A_i := r \begin{pmatrix} \cos \eta_i + h \sin \eta_i \\ \sin \eta_i - h \cos \eta_i \end{pmatrix}, \quad B_i := r \begin{pmatrix} \cos \eta_i - h \sin \eta_i \\ \sin \eta_i + h \cos \eta_i \end{pmatrix}, \quad M_i := r(1 - \tau) \begin{pmatrix} \cos \eta_i \\ \sin \eta_i \end{pmatrix}.$$

We obtain $\mathcal{N}_{r,d}$ as follows (see Figure 6):

- the points A_i, B_i and M_i , for $i = 1, 2, 3$, belong to $\partial\mathcal{N}$;
- $\widehat{B_1M_3}$ and $\widehat{M_1A_3}$ are diametrically opposed arcs of the same circle of diameter d , the same for the pairs $\widehat{B_2M_1}$ and $\widehat{M_2A_1}$, $\widehat{M_3B_3}$ and $\widehat{M_3A_2}$;
- the boundary contains the segments $\overline{A_iB_i}$, for $i = 1, 2, 3$, and the contact point I_i with the incircle is the middle of the corresponding segment.

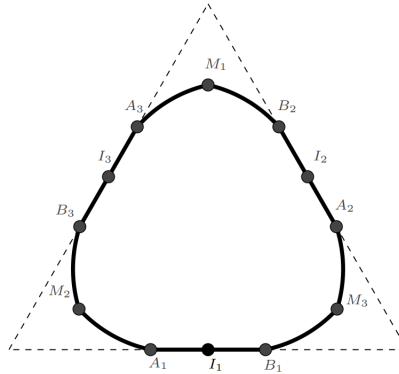


FIGURE 6. A smoothed regular nonagon.

Let us now recall some sharp inequalities that we will need in the sequel. Those classic estimates are obtained via the study of Blaschke–Santaló diagrams involving the following geometric quantities: the perimeter, the area, the inradius, the circumradius, the diameter and the minimal width.

Firstly, let us consider the diagram (A, d, r) . We have the following two theorems.

Theorem 2.17 ([24] and [13]). *Let $\Omega \in \mathcal{K}^2$. We have*

$$(14) \quad |\Omega| \geq r(\Omega) \sqrt{d^2(\Omega) - 4r^2(\Omega)} + r^2(\Omega) \left(\pi - 2 \arccos \left(\frac{2r(\Omega)}{d(\Omega)} \right) \right),$$

where the equality holds if and only if Ω is a two-cup body.

Theorem 2.18 ([13], Theorem 2). *Let $\Omega \in \mathcal{K}^2$. We have*

$$(15) \quad |\Omega| \leq \psi(d(\Omega), r(\Omega)),$$

where

$$(16) \quad \psi(d, r) := \begin{cases} \frac{3\sqrt{3}r}{2}(\sqrt{d^2 - 3r^2} - r) + \frac{3d^2}{2} \left(\frac{\pi}{3} - \arccos \left(\frac{\sqrt{3}r}{d} \right) \right), & \text{if } d \leq rD^* \\ r\sqrt{d^2 - 4r^2} + \frac{d^2}{2} \arcsin \left(\frac{2r}{d} \right), & \text{if } d \geq rD^* \end{cases}$$

and D^* is the unique number in $[2, 2\sqrt{3}]$ for which the two expressions of the function $\psi(d, 1)$ are equal, i.e.,

$$\frac{3\sqrt{3}}{2}(\sqrt{(D^*)^2 - 3} - 1) + \frac{3(D^*)^2}{2} \left(\frac{\pi}{3} - \arccos \left(\frac{\sqrt{3}}{D^*} \right) \right) = \sqrt{(D^*)^2 - 4} + \frac{(D^*)^2}{2} \arcsin \left(\frac{2}{D^*} \right).$$

Moreover, if $d(\Omega) \leq r(\Omega)D^*$, we have the equality in (15) if and only if Ω is a regular smoothed nonagon, while, if $d(\Omega) > r(\Omega)D^*$, we have the equality if and only if Ω is a symmetrical spherical slice.

As far as the diagram (A, ω, R) is concerned, we recall the following theorems:

Theorem 2.19 ([24], Theorem 3). *Let $\Omega \in \mathcal{K}^2$. Then, it holds*

$$(17) \quad |\Omega| \leq \chi(\omega(\Omega), R(\Omega)),$$

where

$$(18) \quad \chi(\omega(\Omega), R(\Omega)) := \frac{\omega(\Omega)}{2} \sqrt{4R(\Omega)^2 - \omega(\Omega)^2} + 2R(\Omega)^2 \arcsin \frac{\omega(\Omega)}{2R(\Omega)},$$

and the equality in (17) holds if and only if Ω is a symmetrical spherical slice.

Theorem 2.20 ([24], Theorem 6). *Let $\Omega \in \mathcal{K}^2$. Then, if $\omega(\Omega) \leq \frac{3}{2}R(\Omega)$, it holds*

$$(19) \quad 16|\Omega|^6 \geq R^2(\Omega)\omega^2(\Omega) \left(16|\Omega|^4 - R^2(\Omega)\omega^6(\Omega) \right)$$

and the equality holds if and only if Ω is a subequilateral triangle.

We recall the following inequality from the diagram (R, r, ω) .

Theorem 2.21 ([23], Theorem 2). *Let $\Omega \in \mathcal{K}^2$. Then, it holds*

$$(20) \quad (4r(\Omega) - \omega(\Omega))(\omega(\Omega) - 2r(\Omega)) \leq \frac{2r^3(\Omega)}{R(\Omega)}$$

and the equality holds if and only if Ω is an isosceles triangle.

Theorem 2.22 ([36], Section 10). *Let $\Omega \in \mathcal{K}^2$. Then, it holds*

$$(21) \quad \omega(\Omega) \leq R(\Omega) + r(\Omega),$$

where the equality is achieved by any set of constant width (i.e., the set Ω is such that the function ω_Ω , defined in Definition 2.5, is constant).

The following theorem deals with the (A, r, R) diagram.

Theorem 2.23 ([24], Theorems 1 and 2). *Let $\Omega \in \mathcal{K}^2$. Then, it holds*

$$(22) \quad |\Omega| \geq 2r(\Omega) \left(\sqrt{R(\Omega)^2 - r(\Omega)^2} + r \arcsin \frac{r(\Omega)}{R(\Omega)} \right),$$

and the equality in (22) holds if and only if Ω is a two-cup body. Moreover, we have

$$(23) \quad |\Omega| \leq \varphi(R(\Omega), r(\Omega)),$$

where

$$(24) \quad \varphi(R(\Omega), r(\Omega)) := 2 \left(r \sqrt{R(\Omega)^2 - r(\Omega)^2} + R^2(\Omega) \arcsin \frac{r(\Omega)}{R(\Omega)} \right),$$

and the equality in (24) holds if and only if Ω is a symmetrical spherical slice.

Now we quote two inequalities concerning the (A, ω, r) and (P, ω, r) diagrams.

Theorem 2.24 ([24], Theorem 5). *Let $\Omega \in \mathcal{K}^2$. We have*

$$(25) \quad (\omega(\Omega) - 2r(\Omega))^2 (4r(\Omega) - \omega(\Omega)) |\Omega|^2 \leq r^4(\Omega) \omega^3(\Omega)$$

and

$$(26) \quad (\omega(\Omega) - 2r(\Omega))^2 (4r(\Omega) - \omega(\Omega)) P^2(\Omega) \leq 4r(\Omega)^2 \omega^3(\Omega)$$

In both inequalities, the equality holds if and only if Ω is a subequilateral triangle.

Finally, we recall this result from the (d, ω, r) diagram.

Theorem 2.25 ([21], Theorem 1-2). *Let $\Omega \in \mathcal{K}^2$. We have*

$$(27) \quad d^2(\Omega) (\omega(\Omega) - 2r(\Omega))^2 (4r(\Omega) - \omega(\Omega)) \leq 4r^4(\Omega) \omega(\Omega),$$

where the equality holds if and only if Ω is a subequilateral triangle T_I , and

$$(28) \quad \omega(\Omega) - r(\Omega) \leq \frac{\sqrt{3}}{3} d(\Omega),$$

where the equality holds if Ω is a Yamanouti set.

2.3. Inequalities relating the Cheeger constant to one geometric quantity. In the following paragraph, we state the inequalities relating the Cheeger constant to one of the geometric quantities taken into account, obtained by combining classical results.

Proposition 2.26. *Let $\Omega \in \mathcal{K}^2$. We have*

- (1) $h(\Omega) \geq 2\sqrt{\frac{\pi}{|\Omega|}}.$
- (2) $h(\Omega) \geq \frac{4\pi}{P(\Omega)}.$
- (3) $h(\Omega) \geq \frac{4}{d(\Omega)}.$
- (4) $\frac{1}{r(\Omega)} \leq h(\Omega) \leq \frac{2}{r(\Omega)}.$
- (5) $h(\Omega) \geq \frac{2}{R(\Omega)}.$

In (1) – (2) – (3) – (5), the equality is achieved by balls, while the one in the upper bound in (4) is achieved by balls and the lower bound is asymptotically an equality for thinning vanishing stadiums.

Proof. • We have, by using the isoperimetric inequality $P(E) \geq 2\sqrt{\pi|E|}$,

$$(29) \quad h(\Omega) = \inf_{\substack{E \text{ is measurable} \\ E \subset \Omega, |E| > 0}} \frac{P(E)}{|E|} \geq \inf_{\substack{E \text{ is measurable} \\ E \subset \Omega, |E| > 0}} \frac{2\sqrt{\pi}\sqrt{|E|}}{|E|} = \inf_{\substack{E \text{ is measurable} \\ E \subset \Omega, |E| > 0}} \frac{2\sqrt{\pi}}{\sqrt{|E|}} = \frac{2\sqrt{\pi}}{\sqrt{|\Omega|}}.$$

- By using (29) and the isoperimetric inequality, we have

$$h(\Omega) \geq \frac{2\sqrt{\pi}}{\sqrt{|\Omega|}} \geq \frac{4\pi}{P(\Omega)}.$$

- By using (29) and the isodiametric inequality $|\Omega| \leq \frac{\pi}{4}d(\Omega)^2$, we have

$$h(\Omega) \geq \frac{2\sqrt{\pi}}{\sqrt{|\Omega|}} \geq \frac{2\sqrt{\pi}}{\sqrt{\frac{\pi}{4}d(\Omega)^2}} = \frac{4}{d(\Omega)}.$$

- For the upper bound, we have

$$h(\Omega) = \inf_{\substack{E \text{ is measurable} \\ E \subset \Omega, |E| > 0}} \frac{P(E)}{|E|} \leq \frac{P(B_{r(\Omega)})}{|B_{r(\Omega)}|} = \frac{2}{r(\Omega)},$$

where $B_{r(\Omega)}$ is a ball of radius $r(\Omega)$ inscribed in Ω . As, for the lower bound, we have

$$h(\Omega) = \inf_{\substack{E \text{ is measurable} \\ E \subset \Omega, |E| > 0}} \frac{P(E)}{|E|} \geq \inf_{\substack{E \text{ is measurable} \\ E \subset \Omega, |E| > 0}} \frac{1}{r(E)} \geq \frac{1}{r(\Omega)},$$

where we use the inequalities $|E| < r(E)P(E)$ (see [38]) and $r(E) \leq r(\Omega)$.

- By using (29) and the inequality $|\Omega| \leq \pi R(\Omega)^2$ (see [38]), we have

$$h(\Omega) \geq \frac{2\sqrt{\pi}}{\sqrt{|\Omega|}} \geq \frac{2}{R(\Omega)}.$$

□

3. NUMERICAL RESULTS AND BLASCHKE–SANTALÓ DIAGRAMS

In this Section, we introduce numerical tools, that we use to obtain more information on the diagrams and state some conjectures.

3.1. Generation of random convex polygons. We want to provide a numerical approximation of the diagrams studied in Section 5. To do so, a natural idea is to generate a large number of convex bodies (more precisely convex polygons). Subsequently, for each of these sets, we calculate the involved functionals. Nevertheless, the task of (properly) generating random convex polygons is quite challenging and of intrinsic interest. The main difficulty is that one wants to design an efficient and fast algorithm that allows to obtain a uniform distribution of the generated random convex polygons. For clarity, let us discuss two different (naive) approaches:

- one easy way to generate random convex polygons is by rejection sampling. We generate a random set of points in a square; if they form a convex polygon, we return it, otherwise we try again. Unfortunately, the probability of a set of n points uniformly generated inside a given square to be in convex position is equal to $p_n = \left(\frac{\binom{2n-2}{n-1}}{n!}\right)^2$, see [41]. Thus, the random variable X_n corresponding to the expected number of iterations needed to obtain a convex distribution follows a geometric law of parameter p_n , which means that its expectation is given by $\mathbb{E}(X_n) = \frac{1}{p_n} = \left(\frac{n!}{\binom{2n-2}{n-1}}\right)^2$. For example, if $N = 20$, the expected number of iterations is approximately equal to $2 \cdot 10^9$, and, since one iteration is performed in

an average of 0.7 seconds, this means that the algorithm will need about 50 years to provide one convex polygon with 20 sides;

- another natural approach is to generate random points and take their convex hull. This method is quite fast, as one can compute the convex hull of N points in a $\mathcal{O}(N \log(N))$ time (see [2] for example), but it is not quite relevant since it yields to a biased distribution.

In order to avoid the issues stated above, we use an algorithm presented in [35], that is based on the work of P. Valtr [41], where the author computes the probability of a set of n points uniformly generated inside a given square to be in convex position. The author remarks (in Section 4) that the proof yields a fast and non-biased method to generate random convex sets inside a given square. We also refer to [35] for a nice description of the steps of the method and a beautiful animation where one can follow each step; one can also find an implementation of Valtr's algorithm in Java that we decided to translate in Matlab.

To obtain an approximation of the Blaschke–Santaló diagram, we generate 100.000 random convex polygons of unit area and number of sides between 3 and 30, for which we compute the involved functionals. We then obtain clouds of dots that provide approximations of the diagrams. This approach has been used in several works, we refer for example to [3], [14] and [18]. For a new and efficient method of the approximation of Blaschke–Santaló diagrams based on centroidal Voronoi tessellations, we refer to the recent work [7].

3.2. About the computation of the functionals. Let us give few details on the numerical computation of the functionals involved in the paper.

- The **Cheeger constant** is computed by using a code implemented by Benjamin Bogosel in [6] based on the characterization of the Cheeger sets of planar convex sets given in [27] and the **Clipper** toolbox, a very good implementation of polygon offset computation by Agnus Johnson.
- The **inradius** is also computed by using the **Clipper** toolbox and the fact that $r(\Omega)$ is the smallest solution to the equation $|\Omega_t| = 0$.
- The **diameter** is computed via a fast method of computation, which consists in finding all antipodal pairs of points and looking for the diametrical one between them. This is classically known as Shamos algorithm [34].
- The **area** is computed by using Matlab's function "**polyarea**".
- The **minimum width** of a polygon Ω of vertices $\{A_1, \dots, A_N\}$ is computed by using the following formula

$$\omega(\Omega) = \min_{i \in \llbracket 1, N \rrbracket} \max_{j \in \llbracket 1, N \rrbracket} \text{dist}(A_j, (A_i A_{i+1})),$$

where $\text{dist}(A_j, (A_i A_{i+1}))$ corresponds to the distance between the point A_j and the line $(A_i A_{i+1})$ (with the convention $A_{N+1} := A_1$).

- The **circumradius** of a convex set Ω can be written as follows

$$R(\Omega) = \min_{c \in \Omega} \max_{x \in \Omega} \|c - x\|.$$

It is computed by using Matlab's routine "**fminmax**".

4. PROOF OF THE MAIN RESULTS

4.1. Proof of Theorem 1.1. We start this Section by proving the existence results stated in Theorem 1.1.

Proof of the existence. Let us consider the minimization problem of the Cheeger constant in the classes of sets (1) – (13); the maximization problem can be dealt with similarly.

For all of these classes of sets, in order to prove the existence of the solution, we consider a minimizing sequence $(\Omega_k)_{k \in \mathbb{N}}$ and we prove that it satisfies the hypothesis of the Blaschke Selection Theorem (see [37, Theorem 1.8.7]), that is to say, its boundedness up to translations. Concerning the class of sets involving a diameter or a circumradius constraint, it is clear that, up to a translation, the minimizing sequence is contained in a sufficiently big ball. So it remains to study the problem in $\mathcal{K}_{P,r}^2$, $\mathcal{K}_{\omega,A}^2$, $\mathcal{K}_{r,\omega}^2$ and $\mathcal{K}_{\omega,P}^2$. Concerning $\mathcal{K}_{P,r}^2$,

and $\mathcal{K}_{\omega,P}^2$, we know from [38] that $P = P(\Omega_k) > 2d(\Omega_k)$, for every k , so the sequence of the diameters $d(\Omega_k)$ is equibounded and, consequently, there exists a sufficiently big ball containing the sequence $(\Omega_k)_k$. As far as $\mathcal{K}_{r,\omega}^2$ is concerned, it is possible to prove the boundness of the minimizing sequence whenever $\omega(\Omega_k) > 2r(\Omega_k)$, indeed it holds (see [38])

$$d(\Omega_k) \leq \frac{\omega^2(\Omega_k)}{2(\omega(\Omega_k) - 2r(\Omega_k))}.$$

For the last class $\mathcal{K}_{\omega,A}^2$, from [38], we know that, if $2\omega(\Omega_k) \leq \sqrt{3}d(\Omega_k)$, then

$$2|\Omega_k| \geq \omega(\Omega_k)d(\Omega_k),$$

and, also in this case, the boundedness follows.

So, for every class of sets considered, the Blaschke selection theorem ensures us that, up to a subsequence, (Ω_k) converges with respect to the Hausdorff distance to a convex set Ω^* ; it remains only to prove that this set belongs to the relative class of admissible sets. We observe that all the considered constraints are stable for the Hausdorff convergence. In particular, the stability of the inradius is proved in [13] and the one of the diameter is proved in [20], meanwhile the stability of the area, the perimeter and the width may be found in [37].

It only remains to show that the circumradius is continuous with respect to the Hausdorff distance in the class of admissible sets having a circumradius constraint. Since $R(\Omega_k) = R$, for all $k \in \mathbb{N}$, we have $\Omega_k \subseteq B_R$. Using the stability of the Hausdorff convergence for the inclusion (see [20, Proposition 2.2.17]), we have that $\Omega^* \subseteq B_R$, and consequently $R(\Omega^*) \leq R$. By contradiction, let us suppose that $R(\Omega^*) < R$, so there exists $\bar{R} > 0$ such that $R(\Omega^*) < \bar{R} < R$ and so $\Omega^* \subseteq B_{\bar{R}}$. Therefore, by the Hausdorff convergence, for sufficiently large k , $\Omega_k \subseteq B_{\bar{R}}$, but this would imply $R \leq \bar{R}$, which is absurd.

In order to conclude, we observe that in all the above cases, the set Ω^* cannot be a segment, that is to say, that the minimizing sequence $(\Omega_k)_{k \in \mathbb{N}}$ cannot degenerate losing one dimension. If we are working in a class of sets involving an inradius or width constraint, then, it is clear that, thanks to the continuity of the inradius and width under the Hausdorff convergence, there exists, up to a translation, a sufficiently small ball contained in the minimizing sequence.

Moreover, in the case $\mathcal{K}_{d,A}^2$ and $\mathcal{K}_{R,A}^2$, the non-degeneration is ensured by the continuity of the area under Hausdorff distance and the equiboundedness of the diameter. On the other hand, if we consider the minimization problem in $\mathcal{K}_{R,d}^2$, $\mathcal{K}_{P,d}^2$ and $\mathcal{K}_{P,R}^2$, the inradius can be bounded from below by a positive quantity. In [36, Section 9], it is proved that

$$r(\Omega_k) \geq \frac{d^2(\Omega_k)\sqrt{4R^2(\Omega_k) - d^2(\Omega_k)}}{2R(\Omega_k)(2R(\Omega_k) + \sqrt{4R^2(\Omega_k) - d^2(\Omega_k)})}.$$

In [19, Section 3], it is proved that

$$r(\Omega_k) \geq \frac{P(\Omega_k)}{4} - \frac{d(\Omega_k)}{2},$$

which also yields to

$$r(\Omega_k) \geq \frac{P(\Omega_k)}{4} - R(\Omega_k),$$

as $d(\Omega_k) \leq 2R(\Omega_k)$.

Recalling now that the Cheeger constant is continuous with respect to the Hausdorff convergence when the sets do not degenerate to a segment (see [33, Proposition 3.1]), the existence part of the theorem is proved. \square

4.2. Proof of Theorem 1.2. The following paragraphs of this Section are dedicated to the proof of the explicit bounds and their sharpness.

4.2.1. The triplet (P, h, r) .

Proposition 4.1. *Let $\Omega \in \mathcal{K}^2$. Then, it holds*

$$(30) \quad \frac{1}{r(\Omega)} + \frac{\pi}{P(\Omega) - \pi r(\Omega)} \leq h(\Omega) \leq \frac{1}{r(\Omega)} + \sqrt{\frac{2\pi}{P(\Omega)r(\Omega)}},$$

where the equality is achieved by sets that are homothetic to their form bodies in the upper bound and by the stadiums in the lower bound.

Proof. We combine the following classical convex geometric inequalities that can be found in [38]

$$(31) \quad \frac{P(\Omega)r(\Omega)}{2} \leq |\Omega| \leq r(\Omega)(P(\Omega) - \pi r(\Omega)),$$

with the estimates (2) to obtain the optimal inequalities (30).

The upper bound in (2) is an equality for sets that are homothetic to their form bodies, since both the upper bound in (2) and the lower one in (31) are sharp for such sets.

The lower bound an equality for stadiums, since both the lower bound in (2) and the upper one in (31) are sharp for those sets. \square

4.2.2. *The triplet (d, h, r) .* In the following, we will denote by $\mathcal{S}_{r,d}$ the symmetrical spherical slice of inradius r and diameter d and by $\mathcal{N}_{r,d}$ the regular smoothed nonagon with the same inradius and diameter, see Definitions 2.16 and 2.12.

Proposition 4.2. *Let $\Omega \in \mathcal{K}^2$. Then, it holds*

$$(32) \quad h(\Omega) \leq \frac{1}{r(\Omega)} + \sqrt{\frac{\pi}{r(\Omega)\sqrt{d^2(\Omega) - 4r^2(\Omega)} + r^2(\Omega) \left(\pi - 2 \arccos \left(\frac{2r(\Omega)}{d(\Omega)} \right) \right)}},$$

where the equality is achieved if and only if Ω is a symmetric two-cup body. Moreover, we have

$$(33) \quad h(\Omega) \geq \frac{1}{t_{g_1^\Omega}},$$

where $t_{g_1^\Omega}$ is the smallest solution to the equation

$$(34) \quad g_1^\Omega(t) := \psi(d(\Omega) - 2t, r(\Omega) - t) = \pi t^2$$

on the interval $[0, r(\Omega)]$ and the function ψ is defined in (16).

Moreover, there exists D_0 such that the problem

$$\min\{h(\Omega) \mid \Omega \in \mathcal{K}_{d,r}^2\}$$

is solved by the smoothed nonagon $\mathcal{N}_{r,d}$ if $d < rD_0$ and by the slice $\mathcal{S}_{r,d}$ if $d \geq rD_0$.

Proof. To prove (32), one has just to combine the upper bound in (2), which is an equality for sets that are homothetic to their form bodies, and (14), which is an equality for and only for symmetric two-cup bodies, that are also homothetic to their form bodies.

Let us now prove (33). As in Theorem 2.18 (see [13]), for any constant parameter $r > 0$, we consider the function

$$\Psi_r(x) = \begin{cases} f_r(x) := \frac{3\sqrt{3}r}{2}(\sqrt{x^2 - 3r^2} - r) + \frac{3x^2}{2} \left(\frac{\pi}{3} - \arccos \left(\frac{\sqrt{3}r}{x} \right) \right), & \text{if } x \leq rD^* \\ g_r(x) := r\sqrt{x^2 - 4r^2} + \frac{x^2}{2} \arcsin \left(\frac{2r}{x} \right), & \text{if } x \geq rD^* \end{cases}$$

defined for $x \geq 2r$. The function Ψ_r is strictly increasing. Indeed, we have for every $x < rD^*$

$$f'_r(x) = \frac{3\sqrt{3}rx}{2\sqrt{x^2 - 3r^2}} + 3x \left(\frac{\pi}{3} - \arccos \left(\frac{\sqrt{3}r}{x} \right) \right) - \frac{3\sqrt{3}r}{2\sqrt{1 - \frac{3r^2}{x^2}}} = 3x \left(\frac{\pi}{3} - \arccos \left(\frac{\sqrt{3}r}{x} \right) \right),$$

and for every $x > rD^*$,

$$g'_r(x) = -\frac{r}{\sqrt{1 - \frac{4r^2}{x^2}}} + \frac{rx}{\sqrt{x^2 - 4r^2}} + x \arcsin \left(\frac{2r}{x} \right) = x \arcsin \left(\frac{2r}{x} \right) > 0.$$

Thus, the function f_r is increasing on $[2r, 2\sqrt{3}r]$ and is decreasing on $[2\sqrt{3}r, +\infty)$ and the function g_r is increasing on $[2r, +\infty)$. Moreover, we have by Theorem 2.18 that $D^* \leq 2\sqrt{3}$. So, the function f_r is increasing on the sub-interval $[2r, rD^*]$ and, since $f_r(rD^*) = g_r(rD^*) = \Psi_r(D^*)$, the continuous function Ψ_r is increasing on $[2r, +\infty)$.

Let $t \in [0, r(\Omega)]$, by applying the result of Theorem 2.18 on the convex set Ω_{-t} , we have

$$|\Omega_{-t}| \leq \Psi_{r(\Omega_{-t})}(d(\Omega_{-t})) = \Psi_{r(\Omega)-t}(d(\Omega_{-t})) \leq \Psi_{r(\Omega)-t}(d(\Omega) - 2t) =: g_1^\Omega(t),$$

where, we use the monotonicity of the function $\Psi_{r(\Omega)-t}$ and the estimates (6) and (7).

Now, using Lemma 2.9, we have the following bound for the Cheeger constant

$$(35) \quad h(\Omega) \geq \frac{1}{t_{g_1^\Omega}},$$

where $t_{g_1^\Omega}$ is the smallest solution to the equation $g_1^\Omega(t) = \pi t^2$ on the interval $[0, r(\Omega)]$.

It remains to prove that for every $r > 0$ and $d \geq 2r$, there exists a convex set of inradius r and diameter d such that (35) is an equality. If $d = 2r$ then Ω is a ball and thus the equality is trivial. Let us now consider the following two cases:

- If $d \geq rD^*$, we have, for every $t \in [0, r)$,

$$(36) \quad |(\mathcal{S}_{r,d})_{-t}| = |\mathcal{S}_{r-t,d-2t}| = \Psi_{r-t}(d - 2t),$$

where the first equality is a consequence of the equality $(\mathcal{S}_{r,d})_{-t} = \mathcal{S}_{r-t,d-2t}$ and the second one is a consequence of [13, Theorem 2] and of the following estimate

$$d((\mathcal{S}_{r,d})_{-t}) = d - 2t > rD^* - 2t > rD^* - tD^* = (r - t)D^* = r((\mathcal{S}_{r,d})_{-t})D^*,$$

where we used $D^* \approx 2,3888 > 2$ (see [13, Theorem 2]). Thus, we have by (36)

$$h(\mathcal{S}_{r,d}) = \frac{1}{t_{g_1^\Omega}},$$

with

$$r(\mathcal{S}_{r,d}) = r \quad \text{and} \quad d(\mathcal{S}_{r,d}) = d.$$

- If $d \in (2r, rD^*]$, we consider $t^* := \frac{D^*r-d}{D^*-2}$, that is the value for which the graphs of the functions $t \mapsto |(\mathcal{N}_{r,d})_{-t}|$ and $t \mapsto |(\mathcal{S}_{r,d})_{-t}|$ intersect each other, see Figure 7. We note that $(\mathcal{N}_{r,d})_{-t} = \mathcal{N}_{r-t,d-2t}$ for every $t \in [0, t^*]$.

We introduce the quantity $D_0 \in (2, D^*)$ as the (unique) value in the interval $(2, D^*)$ for which the graph of the (decreasing) function $x \mapsto \frac{D^*-x}{D^*-2}$ intersects the graph of the (increasing¹) one $x \mapsto \frac{1}{h(\mathcal{N}_{1,x})}$. As shown in Figure 7, we have the following cases:

- If $\frac{d}{r} < D_0$, i.e., $t^* > \frac{1}{h(\mathcal{N}_{r,d})}$, we have $h(\mathcal{N}_{r,d}) = \frac{1}{t_{g_1^\Omega}}$, which means that in this case the smoothed nonagon $\mathcal{N}_{r,d}$ provides the equality in (33).

¹The function $x \mapsto \frac{1}{h(\mathcal{N}_{1,x})}$ is increasing because $x \mapsto \mathcal{N}_{1,x}$ is increasing for the inclusion, meanwhile the Cheeger constant is decreasing with respect to the inclusion.

- If $\frac{d}{r} > D_0$, i.e., $t^* < \frac{1}{h(\mathcal{N}_{r,d})}$, we have $h(\mathcal{S}_{r,d}) = \frac{1}{t_{g_1^\Omega}}$, which means that in this case the slice $\mathcal{S}_{r,d}$ provides the equality in (33).
- If $\frac{d}{r} = D_0$, i.e., $t^* = \frac{1}{h(\mathcal{N}_{r,d})}$, we have $h(\mathcal{N}_{r,d}) = h(\mathcal{S}_{r,d}) = \frac{1}{t_{g_1^\Omega}}$, which means that in this case both the smoothed nonagon $\mathcal{N}_{r,d}$ and the slice $\mathcal{S}_{r,d}$ provide the equality in (33).

So, the proof is concluded.

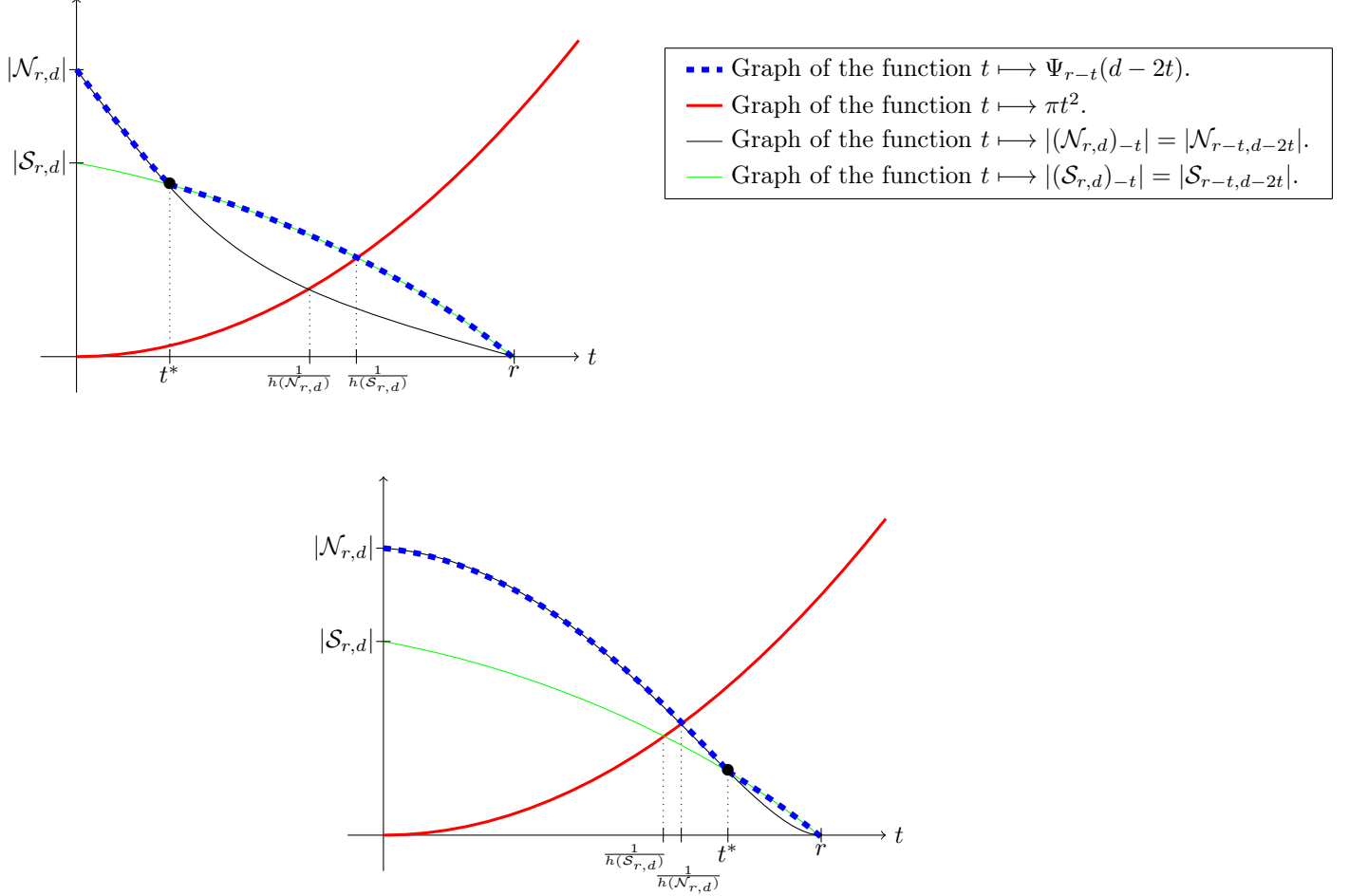


FIGURE 7. Different cases of equality in inequality (33).

□

Remark 4.3. We note that the symmetrical slices and the smoothed nonagons are not the only sets solving the shape optimization problem $\min\{h(\Omega) \mid \Omega \in \mathcal{K}_{d,r}^2\}$. Indeed, if for example we consider a spherical slice \mathcal{S} and denote by $C_{\mathcal{S}}$ its Cheeger set, we have $h(\mathcal{S}) = h(C_{\mathcal{S}})$ and, by the explicit characterization of the Cheeger sets

given in [27, Theorem 1], we have

$$r(C_S) = r\left(\mathcal{S}_{-\frac{1}{h(S)}} + \frac{1}{h(S)}B_1\right) = r\left(\mathcal{S}_{-\frac{1}{h(S)}}\right) + \frac{1}{h(S)} = r(S) - \frac{1}{h(S)} + \frac{1}{h(S)} = r(S)$$

and

$$d(C_S) = d(S),$$

meanwhile $S \neq C_S$, which proves the non-uniqueness of the solution of the minimization problem

$$\min\{h(\Omega) \mid \Omega \in \mathcal{K}_{d,r}^2\}.$$

Remark 4.4. We give the following explicit lower bound. In [38], it is proved that

$$|\Omega| < 2d(\Omega)r(\Omega).$$

By applying the strategy of Lemma 2.9, we obtain that

$$(37) \quad h(\Omega) \geq \frac{4 - \pi}{d(\Omega) + 2r(\Omega) - \sqrt{(d(\Omega) + 2r(\Omega))^2 - 2(4 - \pi)d(\Omega)r(\Omega)}}.$$

This estimate is asymptotically achieved by spherical slices with increasing diameter, as shown in Figure 8.

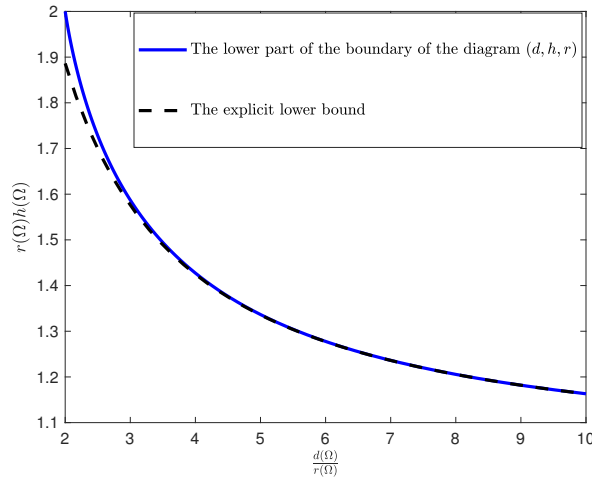


FIGURE 8. The explicit inequality (37) and the lower part of the boundary of the diagram (d, h, r) .

4.2.3. The triplet (R, h, r) .

Proposition 4.5. Let $\Omega \in \mathcal{K}^2$. We have

$$(38) \quad h(\Omega) \geq \frac{1}{t_{g_2^\Omega}},$$

where $t_{g_2^\Omega}$ is the smallest solution of the equation

$$(39) \quad g_2^\Omega(t) := 2 \left((r - t) \sqrt{(R(\Omega) - t)^2 - (r(\Omega) - t)^2} + (R(\Omega) - t)^2 \arcsin \left(\frac{r(\Omega) - t}{R(\Omega) - t} \right) \right) = \pi t^2.$$

The equality in (38) is achieved if and only if Ω is a symmetrical spherical slice. Moreover,

$$(40) \quad h(\Omega) \leq \frac{1}{r(\Omega)} + \sqrt{\frac{\pi}{2r(\Omega) \left(\sqrt{R(\Omega)^2 - r(\Omega)^2} + r(\Omega) \arcsin \left(\frac{r(\Omega)}{R(\Omega)} \right) \right)},$$

where the equality in (40) is achieved by two-cup bodies.

Proof. In order to prove (38), we apply the result of Lemma 2.9. Let us introduce the function

$$\varphi : (R, r) \mapsto 2 \left(r \sqrt{R^2 - r^2} + R^2 \arcsin \frac{r}{R} \right),$$

which is increasing with respect to the first variable, indeed

$$\frac{\partial \varphi}{\partial R}(R, r) = 2R \arcsin \left(\frac{r}{R} \right) > 0.$$

By applying (23) (where the equality holds only for symmetrical spherical slices), we have, for every $t \in [0, r(\Omega)]$,

$$|\Omega_{-t}| \leq \varphi(R(\Omega_{-t}), r(\Omega_{-t})) = \varphi(R(\Omega_{-t}), r(\Omega) - t) \leq \varphi(R(\Omega) - t, r(\Omega) - t) =: g_2^\Omega(t),$$

where the last inequality is a consequence of the monotonicity of the function $R \mapsto \varphi(R, r)$ and of the fact that $R(\Omega_{-t}) \leq R(\Omega) - t$ (see Lemma 2.8). Finally, we conclude by applying the result of Lemma 2.9.

In order to prove (40), we combine the upper bound in (2) and inequality (22). As far as the sharpness of (40) is concerned, we observe that (2) is sharp on sets that are homothetic to their form bodies and (22) is attained by symmetric two-cup bodies, that are also sets that are homothetic to their form bodies. \square

Remark 4.6. We have the following explicit lower bound

$$(41) \quad h(\Omega) \geq \frac{4 - \pi}{2(R(\Omega) + r(\Omega)) - \sqrt{4(R(\Omega) + r(\Omega))^2 - 4(4 - \pi)R(\Omega)r(\Omega)}}.$$

The inequality can be obtained by combining

$$|\Omega| \leq 4R(\Omega)r(\Omega),$$

see [19], and the strategy from Lemma 2.9. Moreover, the inequality is asymptotically achieved by spherical slices with increasing circumradius, see Figure 9.

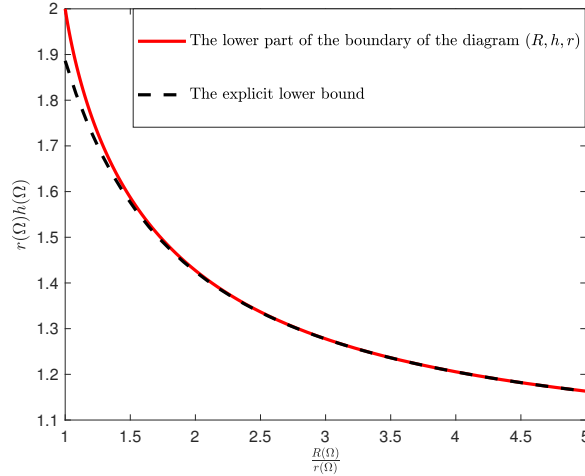


FIGURE 9. The explicit inequality (41) and the lower part of the boundary of the diagram (R, h, r) .

4.3. Explicit description of the Blaschke-Santaló diagrams. We denote by \mathcal{D}_1 , \mathcal{D}_2 and \mathcal{D}_3 the Blaschke Santaló diagram respectively corresponding to the triplets (P, h, r) , (d, h, r) and (R, h, r) . We have defined the quantities $t_{g_1^\Omega}$ and $t_{g_2^\Omega}$ respectively as the smallest solution on $[0, r(\Omega)]$ of equations (34) and (39). We observe that $t_{g_1^\Omega}$ depends on $r(\Omega)$ and $d(\Omega)$, and $t_{g_2^\Omega}$ depends on $r(\Omega)$ and $R(\Omega)$.

In the following proposition, we are keeping the inradius $r(\Omega) = 1$ and consider different values of the remaining variables: diameter for the diagram \mathcal{D}_2 and circumradius for \mathcal{D}_3 . We then use the notation:

$$t_{g_1^\Omega} = t_{g_1}(x) \text{ when } d(\Omega) = x \text{ and } t_{g_2^\Omega} = t_{g_2}(x) \text{ when } R(\Omega) = x.$$

Proposition 4.7. *We obtain the following description of the Blaschke-Santaló diagrams*

$$(42) \quad \mathcal{D}_1 := \{(P(\Omega), h(\Omega)) \mid \Omega \in \mathcal{K}^2, r(\Omega) = 1\} = \left\{ (x, y) \mid x \geq 2\pi \text{ and } 1 + \frac{\pi}{x - \pi} \leq y \leq 1 + \sqrt{\frac{2\pi}{x}} \right\}.$$

$$(43) \quad \mathcal{D}_2 := \{(R(\Omega), h(\Omega)) \mid \Omega \in \mathcal{K}^2, r(\Omega) = 1\} = \left\{ (x, y) \mid x \geq 1 \text{ and } \frac{1}{t_{g_2}(x)} \leq y \leq 1 + \sqrt{\frac{\pi}{2(\sqrt{x^2 - 1} + \arcsin \frac{1}{x})}} \right\}.$$

$$(44) \quad \mathcal{D}_3 := \{(d(\Omega), h(\Omega)) \mid \Omega \in \mathcal{K}^2, r(\Omega) = 1\} = \left\{ (x, y) \mid x \geq 2 \text{ and } \frac{1}{t_{g_1}(x)} \leq y \leq 1 + \sqrt{\frac{\pi}{\sqrt{x^2 - 4} + (\pi - 2 \arccos \frac{2}{x})}} \right\}.$$

Proof. • The diagram \mathcal{D}_1 of the triplet (P, h, r) :

Let us prove that (42) holds. The bounds proved in Proposition 4.1 ensure that

$$\mathcal{D}_1 \subseteq \left\{ (x, y) \mid x \geq 2\pi \text{ and } 1 + \frac{\pi}{x - \pi} \leq y \leq 1 + \sqrt{\frac{2\pi}{x}} \right\} =: \mathcal{P}.$$

It remains to prove the converse inclusion. First, we observe that the boundary of \mathcal{P} is included in \mathcal{D}_1 . Indeed, we can explicitly construct a family of convex sets which fill the lower part of the boundary of \mathcal{P} : let us consider the family of stadiums $\{R_l\}_{l \geq 0}$ obtained as the convex hull of two balls of radius 1 and centered in $(0, -l/2)$ and $(0, l/2)$. We have

$$P(R_l) = 2\pi + 2l, \quad r(R_l) = 1 \text{ and } h(R_l) = \frac{P(R_l)}{|R_l|} = \frac{2\pi + 2l}{\pi + 2l} = 1 + \frac{\pi}{P(R_l) - \pi}.$$

Let us now construct a family of convex sets filling the upper part of the boundary of \mathcal{P} . We consider the family of two-cup bodies $\{C_k\}_{k \geq 1}$ obtained as the convex hull of the ball B_1 centered at the origin and the points $(-k, 0)$ and $(k, 0)$. By [24], we have

$$P(C_k) = 2 \left(\sqrt{4k^2 - 4} + 2 \arcsin \frac{1}{k} \right), \quad r(C_k) = 1 \text{ and } |C_k| = \left(\sqrt{4k^2 - 4} + 2 \arcsin \frac{1}{k} \right)$$

and, as it is shown in [14],

$$h(C_k) = \frac{1}{r(C_k)} + \sqrt{\frac{\pi}{|C_k|}} = 1 + \sqrt{\frac{2\pi}{P(C_k)}}.$$

In order to conclude, we show that the diagram \mathcal{D}_1 is vertically convex, i.e., that we can always construct continuous and vertical paths included in the diagram and connecting the upper and the lower parts of the boundary of \mathcal{D}_1 , covering, in this way, all the area between the two curves.

Let $x_0 \geq 2\pi$. There exist $R_{l_0} \in \{R_l\}$ and $C_{k_0} \in \{C_k\}$ such that $P(R_{l_0}) = P(C_{k_0}) = x_0$. Let us define, via the Minkowski sum, the set

$$K_t = tR_{l_0} + (1 - t)C_{k_0}.$$

By the linearity of the perimeter with respect to the Minkowski sum, we have

$$\forall t \in [0, 1], \quad P(K_t) = P(tR_{l_0} + (1-t)C_{k_0}) = tP(R_{l_0}) + (1-t)P(C_{k_0}) = tx_0 + (1-t)x_0 = x_0.$$

As for the inradius, let us consider the unit ball B_1 centred at the origin and the rectangle Q of vertices $(-M, -1)$, $(-M, 1)$, $(M, 1)$ and $(M, -1)$, where $M > 0$ is sufficiently large such that both R_{l_0} and C_{k_0} are contained in Q . We then have for any $t \in [0, 1]$,

$$B_1 \subset tR_{l_0} + (1-t)C_{k_0} \subset Q,$$

which yields by the monotonicity of the inradius with respect to inclusions to

$$\forall t \in [0, 1], \quad 1 = r(B_1) \leq r(tR_{l_0} + (1-t)C_{k_0}) \leq r(Q) = 1.$$

Thus,

$$\forall t \in [0, 1], \quad r(K_t) = 1.$$

On the other hand, by the continuity of the Cheeger constant with respect to the Hausdorff distance, we have by the intermediate value theorem

$$[h(R_{l_0}), h(C_{k_0})] \subset \{h(K_t) \mid t \in [0, 1]\}.$$

Thus, since $\{h(K_t) \mid t \in [0, 1]\} \subset [h(R_{l_0}), h(C_{k_0})]$ (because R_{l_0} and C_{k_0} respectively correspond to points laying on the lower and the upper parts of the boundary of the diagram \mathcal{D}_1), we have the equality

$$[h(R_{l_0}), h(C_{k_0})] = \{h(K_t) \mid t \in [0, 1]\}.$$

This proves that the diagram \mathcal{D}_1 is vertically convex and that $\mathcal{D}_1 = \mathcal{P}$.

- The diagram \mathcal{D}_2 of the triplet (R, h, r) :

The proof of (43) follows the same scheme. Indeed, one can prove that the diagram is vertically convex by considering vertical paths constructed via the Minkowski sums of the extremal sets (those corresponding to points laying on the upper and lower parts of the boundary of the diagram). In the present case, by Proposition 4.5, the upper boundary is filled by points corresponding to two-cup bodies $(C_x)_{x \geq 1}$ such that $R(C_x) = x$ and $r(C_x) = 1$, for all $x \geq 1$. Meanwhile, the lower boundary is filled by points corresponding to spherical slices $(S_x)_{x \geq 1}$ such that $R(S_x) = x$ and $r(S_x) = 1$, for all $x \geq 1$. If one assumes (without loss of generality) that for all $x \geq 1$, both C_x and S_x are centered at the origin and that their diameters are colinear, then, it is clear that $C_x \subset S_x$. Thus, it is straightforward that $C_x \subset (1-t)C_x + tS_x \subset S_x$, for all $t \in [0, 1]$. Therefore, we have by the monotonicity of the circumradius and the inradius with respect to inclusions that

$$\forall t \in [0, 1], \quad 1 = r(C_x) \leq r((1-t)C_x + tS_x) \leq r(S_x) = 1$$

and

$$\forall t \in [0, 1], \quad x = R(C_x) \leq R((1-t)C_x + tS_x) \leq R(S_x) = x.$$

Thus,

$$\forall t \in [0, 1], \quad r((1-t)C_x + tS_x) = 1 \quad \text{and} \quad R((1-t)C_x + tS_x) = x,$$

which allows to conclude the vertical convexity of the diagram as in the previous case.

- The diagram \mathcal{D}_3 of the triplet (d, h, r) :

As for the proof of (44), let $x_0 \geq 2$ and C_{x_0} be a two-cup body such that $r(C_{x_0}) = 1$ and $d(C_{x_0}) = x_0$ (corresponding to a point on the upper boundary of \mathcal{D}_3 , see Proposition 4.2) and L_{x_0} be an extremal shape corresponding to a point on the lower boundary such that $r(C_{x_0}) = 1$ and $d(C_{x_0}) = x_0$. In this case, we have to be more careful as we should distinguish two cases:

- If $x_0 \geq D_0$, then by Proposition 4.2, L_{x_0} is a symmetrical spherical slice whose diameter can be assumed to be colinear to the diameter of C_{x_0} . In this case, we can conclude exactly as in the previous case by considering the convex Minkowski combination of C_{x_0} and L_{x_0} .
- If $x_0 \in [2, D_0)$, then L_{x_0} can be taken as a smoothed nonagon of inradius 1 and diameter x_0 (see Proposition 4.2). In this case, the Minkowski sum does no longer allow to construct a vertical line included in the diagram and joining the upper and the lower parts of its boundary. Therefore, to prove the vertical convexity, we use the following construction introduced in [13, Section 1.2]: Starting from the smoothed nonagon L_{x_0} , we fix one of its diameter, say $[A, B]$ and we shrink continuously L_{x_0} to the set L_{AB} defined as the convex hull of the points A, B and the disk of radius 1 contained in L_{x_0} . Then, we continuously move the points A and B to the points A_0 and B_0 at distance x_0 , oppositely located with respect to the center of the disk (in the sense that the center is the middle of $[A_0, B_0]$) by keeping the convex hull with the disk through the perturbation process, obtaining the two-cup body C_{x_0} as a final shape. By doing so, we constructed a continuous family of convex shapes (of inradius 1 and diameter x_0) connecting L_{x_0} and C_{x_0} , yielding a vertical and continuous line connecting the upper and the lower parts of the boundary of the Blaschke–Santaló diagram \mathcal{D}_3 .

□

Remark 4.8. *As observed in this section, proving sharp bounds corresponding to the boundary of the Blaschke–Santaló diagram is not equivalent to completely characterizing it. Indeed, once we managed to identify the boundary, it remains to show that the diagram is simply connected, which can be a difficult task, see for example [3, Conjecture 5], [31, Open problem 2] and [42, Problem 3]. We refer to [18] for a generic method of proof of the simple connectedness of a Blaschke–Santaló diagram.*

5. THE REMAINING DIAGRAMS

For the remaining triplets of shape functionals, we have proved the existence of a maximum and minimum to the relative shape optimization problems (see Theorem 1.1). Moreover, we are able to identify parts of the boundaries of the corresponding Blaschke–Santaló diagrams. In the following, we state and prove the results that we have obtained.

5.1. The triplet (ω, h, d) .

Proposition 5.1. *Let $\Omega \in \mathcal{K}^2$. We have*

$$(45) \quad h(\Omega) \geq \frac{1}{t_{g_3^\Omega}},$$

where $t_{g_3^\Omega}$ is the smallest solution to

$$g_3^\Omega(t) := \frac{\omega(\Omega) - 2t}{2} \sqrt{(d(\Omega) - 2t)^2 - (\omega(\Omega) - 2t)^2} + \frac{(d(\Omega) - 2t)^2}{2} \arcsin\left(\frac{\omega(\Omega) - 2t}{d(\Omega) - 2t}\right) = \pi t^2.$$

The equality in (45) is achieved by symmetrical spherical slices. Moreover,

- if $\omega(\Omega) \leq \frac{\sqrt{3}}{2}d(\Omega)$, we have

$$(46) \quad h(\Omega) \leq h(T_I),$$

where T_I is the subequilateral triangle such that $\omega(T_I) = \omega(\Omega)$ and $d(T_I) = d(\Omega)$. The equality in (46) is achieved by the isosceles triangle T_I ;

- and if $\frac{\sqrt{3}}{2}d(\Omega) \leq \omega(\Omega) \leq d(\Omega)$, we have

$$(47) \quad h(\Omega) \leq \frac{\sqrt{3}}{\sqrt{3}\omega(\Omega) - d(\Omega)} + \sqrt{\frac{2\pi}{\pi\omega(\Omega)^2 - \sqrt{3}d(\Omega)^2 + 6\omega(\Omega)(\tan(\arccos(\frac{\omega(\Omega)}{d(\Omega)})) - \arccos(\frac{\omega(\Omega)}{d(\Omega)})}}.$$

The equality in (47) is achieved by equilateral triangles.

Proof. • Let us start by proving the lower bound (45), by using the strategy given in Lemma 2.9. For every $\Omega \in \mathcal{K}^2$, it holds

$$|\Omega| \leq \frac{\omega(\Omega)}{2} \sqrt{d^2(\Omega) - \omega^2(\Omega)} + \frac{d^2(\Omega)}{2} \arcsin \left(\frac{\omega(\Omega)}{d(\Omega)} \right),$$

see [29, 38], with equality if and only if Ω is a symmetrical spherical slice. If we denote

$$f(d, w) := \frac{w}{2} \sqrt{d^2 - w^2} + \frac{d^2}{2} \arcsin \left(\frac{w}{d} \right),$$

we have

$$\frac{\partial f}{\partial d}(d, w) = d \arcsin \left(\frac{w}{d} \right) > 0 \quad \text{and} \quad \frac{\partial f}{\partial w}(d, w) = \sqrt{d^2 - w^2} > 0.$$

Thus,

$$|\Omega_{-t}| \leq f(d(\Omega_{-t}), \omega(\Omega_{-t})) \leq f(d(\Omega) - 2t, \omega(\Omega) - 2t).$$

Therefore, by using Lemma 2.9, we have

$$h(\Omega) \geq \frac{1}{t_{g_3^\Omega}},$$

where $t_{g_3^\Omega}$ is the smallest solution of

$$g_3^\Omega(t) := f(d(\Omega) - 2t, \omega(\Omega) - 2t) = \pi t^2.$$

- In order to prove the upper bound (46), we consider the following minimization problem for the area in the class of convex sets with given diameter and width, studied in [38] and [39]:

(i) if $2\omega(\Omega) \leq \sqrt{3}d(\Omega)$, then

$$(48) \quad 2|\Omega| \geq \omega(\Omega)d(\Omega),$$

where the equality is achieved by triangles;

(ii) if $\sqrt{3}d(\Omega) \leq 2\omega(\Omega) \leq 2d(\Omega)$, then

$$(49) \quad 2|\Omega| \geq \pi\omega^2(\Omega) - \sqrt{3}d^2(\Omega) + 6\omega^2(\Omega) \left(\tan \left(\arccos \left(\frac{\omega(\Omega)}{d(\Omega)} \right) \right) - \arccos \left(\frac{\omega(\Omega)}{d(\Omega)} \right) \right) = |T_Y|,$$

where the equality is achieved by the Yamanouti set T_Y such that $\omega(T_Y) = \omega(\Omega)$ and $d(T_Y) = d(\Omega)$.

Moreover, if we consider the minimization problem of the inradius in the class of convex sets with given diameter and width, we have from Theorem 2.25

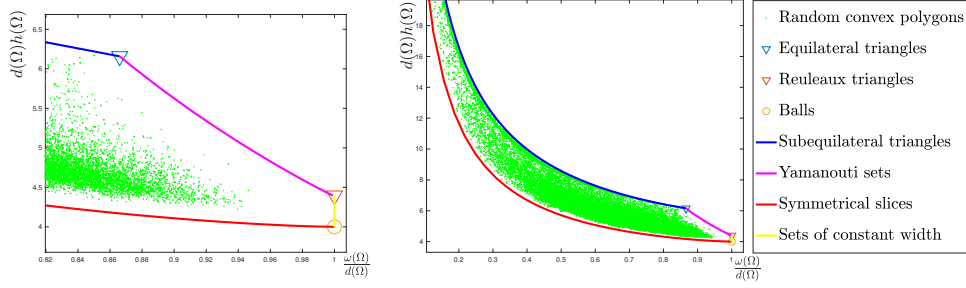
$$(50) \quad r(\Omega) \geq \begin{cases} r(T_I), & \text{if } 2\omega(\Omega) \leq \sqrt{3}d(\Omega), \\ r(T_Y), & \text{if } \sqrt{3}d(\Omega) \leq 2\omega(\Omega) \leq 2d(\Omega). \end{cases}$$

So combining (2) with the estimates (48), (49) and (50), we obtain

$$h(\Omega) \leq \begin{cases} \frac{1}{r(T_I)} + \sqrt{\frac{\pi}{|T_I|}} = h(T_I), & \text{if } 2\omega(\Omega) \leq \sqrt{3}d(\Omega), \\ \frac{1}{r(T_Y)} + \sqrt{\frac{\pi}{|T_Y|}}, & \text{if } \sqrt{3}d(\Omega) \leq 2\omega(\Omega) \leq 2d(\Omega). \end{cases}$$

The explicit formula given in inequality (47) is then obtained by using (49) and $r(T_Y) = \omega(T_Y) - \frac{d(T_Y)}{\sqrt{3}}$, see [21, Theorem 2].

□

FIGURE 10. Blaschke–Santaló diagram of the triplet (ω, h, d) .

We are also able to give an explicit sharp lower bound for the Cheeger constant in terms of the width and the diameter. We note that although being sharp, this inequality does not correspond to a part of the boundary of the Blaschke–Santaló diagram as shown in Figure 11.

Remark 5.2. Let $\Omega \in \mathcal{K}^2$. We have

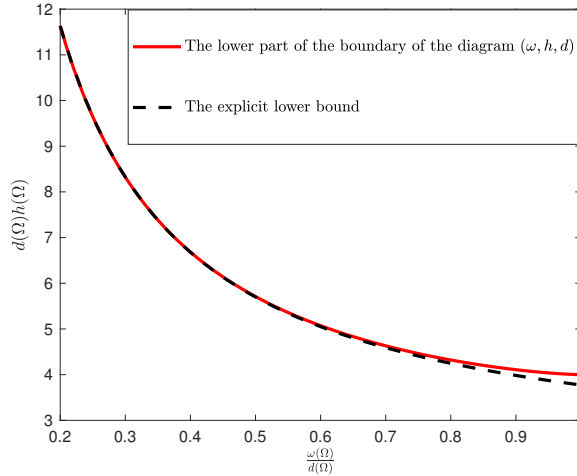
$$(51) \quad h(\Omega) > \frac{1}{\omega(\Omega)} + \frac{1}{d(\Omega)} + \sqrt{\left(\frac{1}{\omega(\Omega)} + \frac{1}{d(\Omega)}\right)^2 - \frac{4 - \pi}{\omega(\Omega)d(\Omega)}},$$

where the equality is asymptotically achieved by a sequence of thin collapsing rectangles or spherical slices as shown in Figure 11.

In order to prove (51), it is enough to consider the inequality

$$|\Omega| \leq \omega(\Omega)d(\Omega)$$

and to use the strategy of Lemma 2.9.

FIGURE 11. The explicit inequality (51) and the lower part of the boundary of the diagram (ω, h, d) .

5.2. The triplet (ω, h, R) .

Proposition 5.3. *Let $\Omega \in \mathcal{K}^2$. We have*

$$(52) \quad h(\Omega) \geq \frac{1}{t_{g_4^\Omega}},$$

where $t_{g_4^\Omega}$ is the smallest solution of the equation

$$g_4^\Omega(t) := \frac{(\omega(\Omega) - 2t)}{2} \sqrt{4(R(\Omega) - t)^2 - (\omega(\Omega) - 2t)^2} + 2(R(\Omega) - t)^2 \arcsin\left(\frac{\omega(\Omega) - 2t}{2(R(\Omega) - t)}\right) = \pi t^2$$

on $[0, r(\Omega)]$. The equality in (52) is achieved by symmetrical spherical slices.

Moreover, if $\omega(\Omega) \leq \frac{3}{2}R(\Omega)$, then

$$(53) \quad h(\Omega) \leq h(T_I),$$

where T_I is the subequilateral triangle such that $R(T_I) = R(\Omega)$ and $\omega(T_I) = \omega(\Omega)$. The equality in (53) is achieved by the subequilateral triangle T_I .

Proof. • Let us start by proving the lower bound (52), by using the strategy given in Lemma 2.9. Let us recall the function defined in (18)

$$\chi : (\omega, R) \mapsto \frac{\omega}{2} \sqrt{4R^2 - \omega^2} + 2R^2 \arcsin \frac{\omega}{2R}.$$

We have, for every $R, \omega > 0$,

$$\frac{\partial \chi}{\partial R}(\omega, R) = 4R \arcsin \frac{\omega}{2R} \geq 0 \quad \text{and} \quad \frac{\partial \chi}{\partial \omega}(\omega, R) = \sqrt{4R^2 - \omega^2} \geq 0.$$

Thus, using Theorem 2.19, we have, for every $t \in [0, r(\Omega)]$,

$$|\Omega_{-t}| \leq \chi(\omega(\Omega_{-t}), R(\Omega_{-t})) \leq \chi(\omega(\Omega) - 2t, R(\Omega) - t) =: g_4^\Omega(t),$$

where we used (8) and (9). By Lemma 2.9, we have

$$h(\Omega) \geq \frac{1}{t_{g_4^\Omega}},$$

where $t_{g_4^\Omega}$ is the smallest solution to the equation $g_4^\Omega(t) = \pi t^2$ on the interval $[0, r(\Omega)]$.

- Let us now prove the upper bound (53). We recall that for all $\Omega \in \mathcal{K}^2$ such that $\omega(\Omega) \leq \frac{3}{2}R(\Omega)$, we have

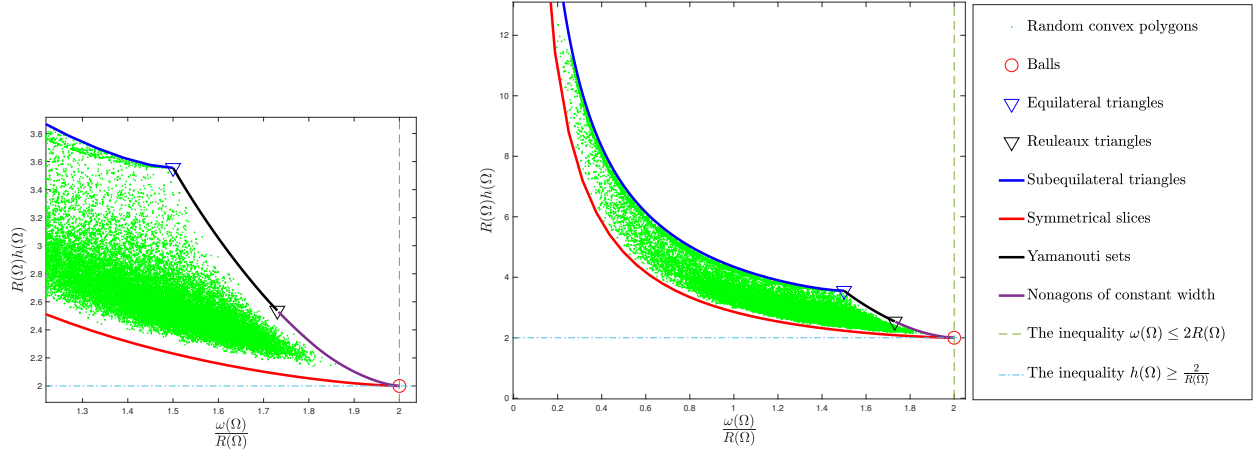
$$|\Omega| \geq |T_I| \quad \text{and} \quad r(\Omega) \geq r(T_I),$$

where T_I is a subequilateral triangle such that $\omega(T_I) = \omega(\Omega)$ and $R(T_I) = R(\Omega)$, see respectively (19) and (20).

To conclude, one just has to combine those estimates with the inequality

$$h(\Omega) \leq \frac{1}{r(\Omega)} + \sqrt{\frac{\pi}{|\Omega|}},$$

see [14], which is an equality for sets that are homothetic to their form bodies, in particular, subequilateral triangles. □

FIGURE 12. Blaschke–Santaló diagram of the triplet (ω, h, R) .

In the following remark, we give some explicit sharp bounds, that do not correspond to parts of the boundary of the Blaschke–Santaló diagram.

Remark 5.4. *We can prove that*

$$(54) \quad h(\Omega) \leq \frac{3}{\omega(\Omega)} + \sqrt{\frac{\pi}{\sqrt{3}R(\Omega)\omega(\Omega)}}.$$

We recall the following inequalities, proved in [38],

$$(55) \quad |\Omega| \geq \sqrt{3}R(\Omega)\omega(\Omega) \quad \text{and} \quad \omega(\Omega) \leq 3r(\Omega).$$

By combining these estimates and the upper bound in (2), we have

$$h(\Omega) \leq \frac{3}{\omega(\Omega)} + \sqrt{\frac{\pi}{\sqrt{3}R(\Omega)\omega(\Omega)}}.$$

Since the equality in (2) is achieved by sets that are homothetic to their form bodies, while the equalities in (55) are achieved by equilateral triangles, that are particular sets that are homothetic to their form bodies, we have the equality in (54) for equilateral triangles.

Moreover, another sharp lower bound can be obtained by using the strategy from Lemma 2.9, starting from

$$|\Omega| < 2R(\Omega)\omega(\Omega),$$

which is asymptotically achieved by a sequence of rectangles or spherical slices with circumradius that goes to infinity (see [19]), as shown in Figure 13. We get $|\Omega_{-t}| \leq 2R(\Omega_{-t})\omega(\Omega_{-t}) \leq 2(R(\Omega) - t)(\omega(\Omega) - 2t)$ and, consequently,

$$(56) \quad h(\Omega) \geq \frac{4 - \pi}{(2R(\Omega) + \omega(\Omega)) - \sqrt{(2R(\Omega) + \omega(\Omega))^2 - (4 - \pi)(2R(\Omega)\omega(\Omega))}}.$$

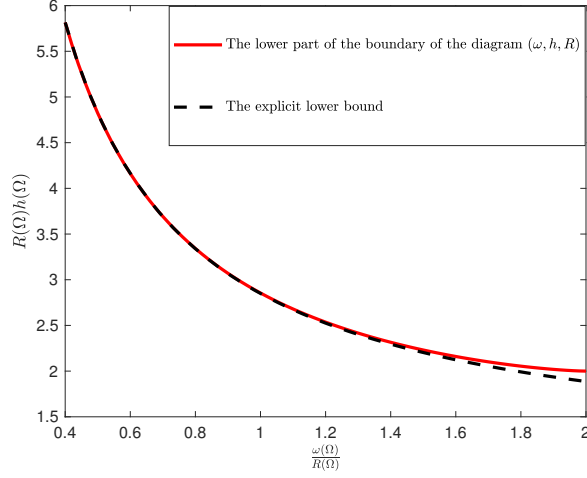


FIGURE 13. The explicit inequality (56) and the lower part of the boundary of the diagram (ω, h, d) .

5.3. The triplet $(\omega, h, |\cdot|)$.

Proposition 5.5. *Let $\Omega \in \mathcal{K}^2$. We have*

$$(57) \quad h(\Omega) \geq \frac{2}{\omega(\Omega)} + \frac{\pi\omega(\Omega)}{2|\Omega|},$$

where the equality is achieved by stadiums. Moreover, we have

$$(58) \quad h(\Omega) \leq h(T_I),$$

where T_I is a subequilateral triangle such that $|\Omega| = |T_I|$ and $\omega(\Omega) = \omega(T_I)$. The equality in (58) is achieved by the subequilateral triangle T_I .

Proof. • Let us prove inequality (57). We recall the lower bound in (2)

$$h(\Omega) \geq \frac{1}{r(\Omega)} + \frac{\pi r(\Omega)}{2|\Omega|},$$

which is an equality if and only if Ω is a stadium. Inequality (57) is then a consequence of the fact that the function $r \mapsto \frac{1}{r} + \frac{\pi r}{2|\Omega|}$ is strictly decreasing and $r(\Omega) \leq \frac{\omega(\Omega)}{2}$ (where the equality holds for stadiums).

• Let us now prove inequality (58). We start by recalling inequality (25):

$$|\Omega| \leq \sqrt{\frac{r^4(\Omega)\omega^3(\Omega)}{(\omega(\Omega) - 2r(\Omega))^2(4r(\Omega) - \omega(\Omega))}} =: f_{\omega(\Omega)}(r(\Omega)).$$

By direct computations, we prove that the continuous function

$$f_{\omega(\Omega)} : r \mapsto \sqrt{\frac{r^4\omega(\Omega)^3}{(\omega(\Omega) - 2r)^2(4r - \omega(\Omega))}}$$

is strictly increasing on $\left[\frac{\omega(\Omega)}{3}, \frac{\omega(\Omega)}{2}\right)$. Let us denote by $g_{\omega(\Omega)}$ the inverse function of $f_{\omega(\Omega)}$, which is also continuous and strictly increasing. We have

$$r(\Omega) \geq g_{\omega(\Omega)}(|\Omega|) = r(T_I),$$

where T_I is any subequilateral triangle such that $\omega(T_I) = \omega(\Omega)$ and $|T_I| = |\Omega|$. Thus, we have

$$h(\Omega) \leq \frac{1}{r(\Omega)} + \sqrt{\frac{\pi}{|\Omega|}} \leq \frac{1}{r(T_I)} + \sqrt{\frac{\pi}{|T_I|}} = h(T_I),$$

with equality if and only if $\Omega = T_I$, where we used the upper bound in (2). □

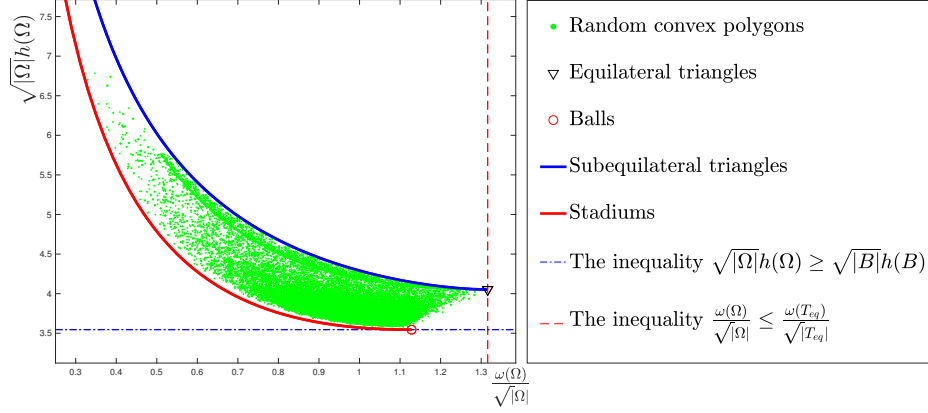


FIGURE 14. Blaschke-Santaló diagram of the triplet $(\omega, h, |\cdot|)$.

Remark 5.6. One may use classical convex geometry inequalities to obtain simpler bounds than the implicit one given in (58). Indeed, if we combine the inequalities in (2) and the following classical ones

$$\frac{2}{\omega(\Omega)} \leq \frac{1}{r(\Omega)} \leq \frac{2}{\omega(\Omega)} + \frac{\omega(\Omega)}{\sqrt{3}|\Omega|},$$

where the lower bound is realized in particular by stadiums, and the upper one by equilateral triangles (see for example [38] and the references therein), we obtain the following inequalities

$$(59) \quad h(\Omega) \leq \frac{2}{\omega(\Omega)} + \frac{\omega(\Omega)}{\sqrt{3}|\Omega|} + \sqrt{\frac{\pi}{|\Omega|}}$$

and

$$(60) \quad h(\Omega) \leq \frac{2}{\omega(\Omega) - \frac{\omega(\Omega)^3}{4|\Omega|}} + \sqrt{\frac{\pi}{|\Omega|}}.$$

The bound (59) is attained for equilateral triangles and (60) is asymptotically attained for a sequence of thin subequilateral triangles.

5.4. The triplet (ω, h, P) .

Proposition 5.7. Let $\Omega \in \mathcal{K}^2$. We have

$$(61) \quad h(\Omega) \geq \frac{2}{\omega(\Omega)} + \frac{2\pi}{2P(\Omega) - \pi\omega(\Omega)},$$

where the equality is achieved by stadiums.

Moreover, if $P(\Omega) \geq 2\sqrt{3}\omega(\Omega)$, then,

$$(62) \quad h(\Omega) \leq h(T_I),$$

where T_I is a subequilateral triangle such that $P(T_I) = P(\Omega)$ and $\omega(T_I) = \omega(\Omega)$. The equality in (62) is achieved by the subequilateral triangle T_I .

Proof. • Inequality (61) is a consequence of (57) and the inequality

$$|\Omega| \leq \frac{\omega(\Omega)}{2} \left(P(\Omega) - \frac{\pi\omega(\Omega)}{2} \right),$$

which is an equality for stadiums, see for example [38].

- Let us now assume that $P(\Omega) \geq 2\sqrt{3}\omega(\Omega)$. In order to prove (62), we recall inequality (26):

$$P(\Omega) \leq \sqrt{\frac{4r^2(\Omega)\omega^3(\Omega)}{(\omega(\Omega) - 2r(\Omega))^2(4r(\Omega) - \omega(\Omega))}} =: f_{\omega(\Omega)}(r(\Omega)).$$

By direct computations, we prove that the continuous function

$$f_{\omega(\Omega)} : r \mapsto \sqrt{\frac{4r^2\omega(\Omega)^3}{(\omega(\Omega) - 2r)^2(4r - \omega(\Omega))}}$$

is strictly increasing on $\left[\frac{\omega(\Omega)}{3}, \frac{\omega(\Omega)}{2}\right)$. Let us denote by $g_{\omega(\Omega)}$ the inverse function of $f_{\omega(\Omega)}$, which is also continuous and strictly increasing. We have

$$r(\Omega) \geq g_{\omega(\Omega)}(P(\Omega)) = r(T_I),$$

where T_I is any subequilateral triangle such that $\omega(T_I) = \omega(\Omega)$ and $P(T_I) = P(\Omega)$. Moreover, since $P(\Omega) \geq 2\sqrt{3}\omega(\Omega)$, we have by the results contained in [43],

$$|\Omega| \geq |T_I|,$$

(see also [38] as a reference). Finally, we obtain

$$h(\Omega) \leq \frac{1}{r(\Omega)} + \sqrt{\frac{\pi}{|\Omega|}} \leq \frac{1}{r(T_I)} + \sqrt{\frac{\pi}{|T_I|}} = h(T_I).$$

□

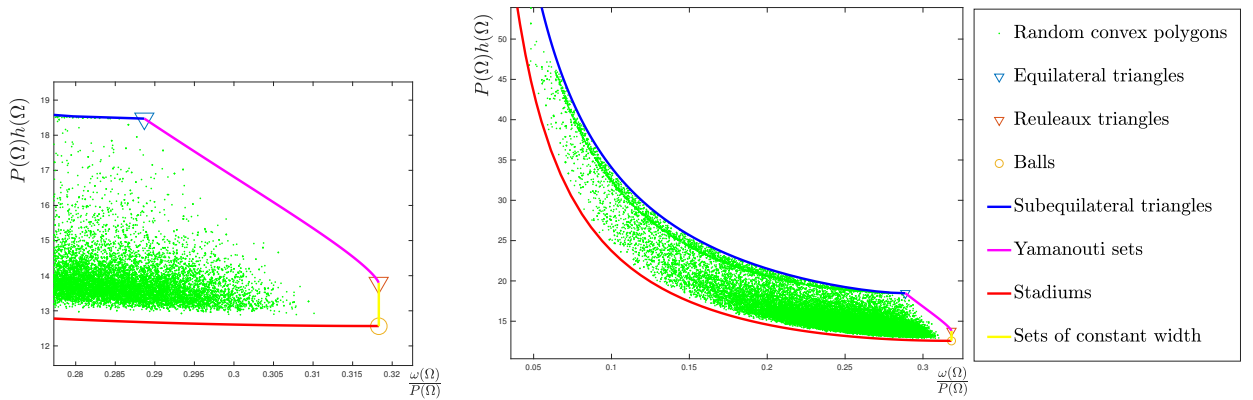


FIGURE 15. Blaschke–Santaló diagram of the triplet (ω, h, P) .

5.5. The triplet (R, h, d) .

Proposition 5.8. *Let $\Omega \in \mathcal{K}^2$. We have*

$$(63) \quad h(\Omega) \leq \frac{2R(\Omega) \left(2R(\Omega) + \sqrt{4R(\Omega)^2 - d(\Omega)^2} \right)}{d(\Omega)^2 \sqrt{4R(\Omega)^2 - d(\Omega)^2}} + \sqrt{\frac{4\pi R(\Omega)^2}{d(\Omega)^3 \sqrt{4R(\Omega)^2 - d(\Omega)^2}}},$$

where the equality is achieved by subequilateral triangles.

Proof. Inequality (63) is obtained by combining

$$h(\Omega) \leq \frac{1}{r(\Omega)} + \sqrt{\frac{\pi}{|\Omega|}},$$

see [14], which is an equality for sets that are homothetic to their form bodies (in particular subequilateral triangles), and

$$|\Omega| \geq \frac{d(\Omega)^3 \sqrt{4R(\Omega)^2 - d(\Omega)^2}}{4R(\Omega)^2} \quad \text{and} \quad r(\Omega) \geq \frac{d(\Omega)^2 \sqrt{4R(\Omega)^2 - d(\Omega)^2}}{2R(\Omega) \left(2R(\Omega) + \sqrt{4R(\Omega)^2 - d(\Omega)^2} \right)},$$

respectively proved in [22] and [36], where the equalities hold only for subequilateral triangles. \square

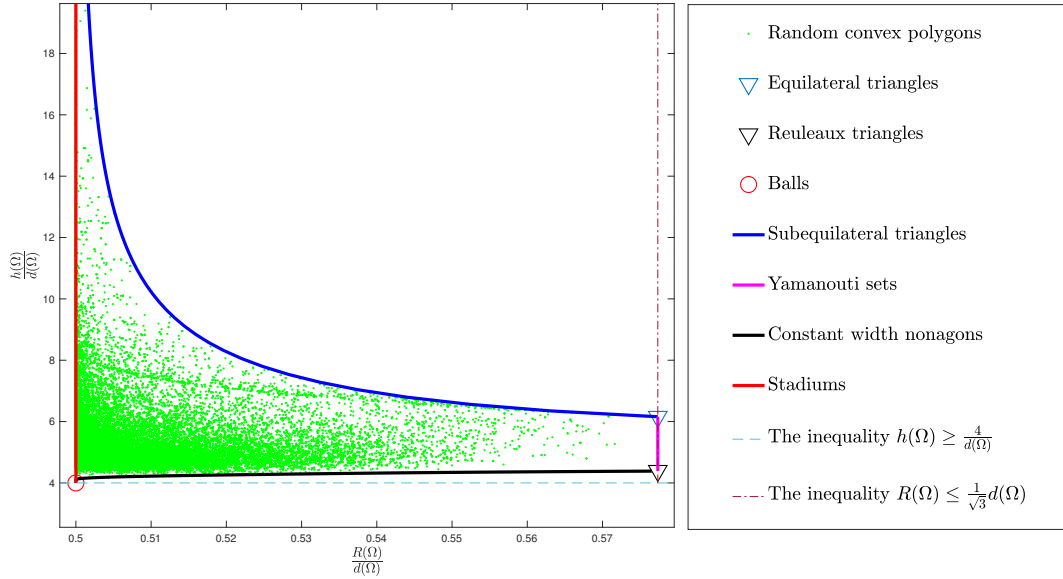


FIGURE 16. Blaschke-Santaló diagram of the triplet (R, h, d) , See Conjecture 3 and Figure 18 for the definition of constant width nonagons.

5.6. The triplet (ω, h, r) .

Proposition 5.9. *Let $\Omega \in \mathcal{K}^2$. We have*

$$(64) \quad h(\Omega) \geq \frac{1}{r(\Omega)} + \frac{1}{r(\Omega)} \sqrt{\pi \left(1 - \frac{2r(\Omega)}{\omega(\Omega)} \right)} \sqrt{\frac{4r(\Omega)}{\omega(\Omega)} - 1},$$

where the equality is achieved by subequilateral triangles.

Proof. The present demonstration is inspired by the proof of [24, Theorem 5].

It is known that the incircle of a set Ω meets the boundary of Ω either in two points contained in two parallel lines, or in (at least) three points that form the vertices of a triangle, see [8]. In the first case, we have $\omega(\Omega) = 2r(\Omega)$, thus inequality (64) is equivalent to $h(\Omega) \geq \frac{1}{r(\Omega)}$, which is proved in Proposition 2.26. In the second case, let us denote by T a triangle formed by three lines of support common to Ω and the incircle. We have $r(\Omega) = r(T)$ and, by $\Omega \subset T$ and the monotonicity with respect to the inclusion, we get

$$(65) \quad h(\Omega) \geq h(T)$$

and

$$(66) \quad \omega(\Omega) \leq \omega(T).$$

So, inequality (64) is equivalent to the following one

$$\frac{1}{r(\Omega)h(\Omega)} f\left(\frac{r(\Omega)}{\omega(\Omega)}\right) \leq 1,$$

where $f : x \in [\frac{1}{3}, \frac{1}{2}] \mapsto 1 + \sqrt{\pi(1-2x)\sqrt{4x-1}}$. We observe that the function $g : x \in [\frac{1}{3}, \frac{1}{2}] \mapsto (1-2x)\sqrt{4x-1}$ is decreasing. Indeed,

$$g'(x) = \frac{4(1-3x)}{\sqrt{4x-1}} \leq 0.$$

Thus, f is also decreasing on $[\frac{1}{3}, \frac{1}{2}]$. Then, since $\frac{r(\Omega)}{\omega(\Omega)} \geq \frac{r(T)}{\omega(T)}$ by (66), we have

$$f\left(\frac{r(\Omega)}{\omega(\Omega)}\right) \leq f\left(\frac{r(T)}{\omega(T)}\right).$$

Moreover, we get by (65),

$$\frac{1}{r(\Omega)h(\Omega)} \leq \frac{1}{r(T)h(T)}.$$

Thus, we obtain

$$\frac{1}{r(\Omega)h(\Omega)} f\left(\frac{r(\Omega)}{\omega(\Omega)}\right) \leq \frac{1}{r(T)h(T)} f\left(\frac{r(T)}{\omega(T)}\right) = \frac{1}{1+r(T)\sqrt{\frac{\pi}{|T|}}} f\left(\frac{r(T)}{\omega(T)}\right),$$

where we used the equality $h(T) = \frac{1}{r(T)} + \sqrt{\frac{\pi}{|T|}}$, which holds because T is a triangle, see [14, Theorem 1.3]. Now, we use the inequality

$$|T| \leq \frac{r(T)^2}{\left(1 - \frac{2r(T)}{\omega(T)}\right) \sqrt{\frac{4r(T)}{\omega(T)} - 1}},$$

which is an equality if and only if T is a subequilateral triangle, see [24, Theorem 5]. We then have

$$\frac{1}{r(\Omega)h(\Omega)} f\left(\frac{r(\Omega)}{\omega(\Omega)}\right) \leq \frac{1}{1+r(T)\sqrt{\frac{\pi}{|T|}}} f\left(\frac{r(T)}{\omega(T)}\right) \leq 1,$$

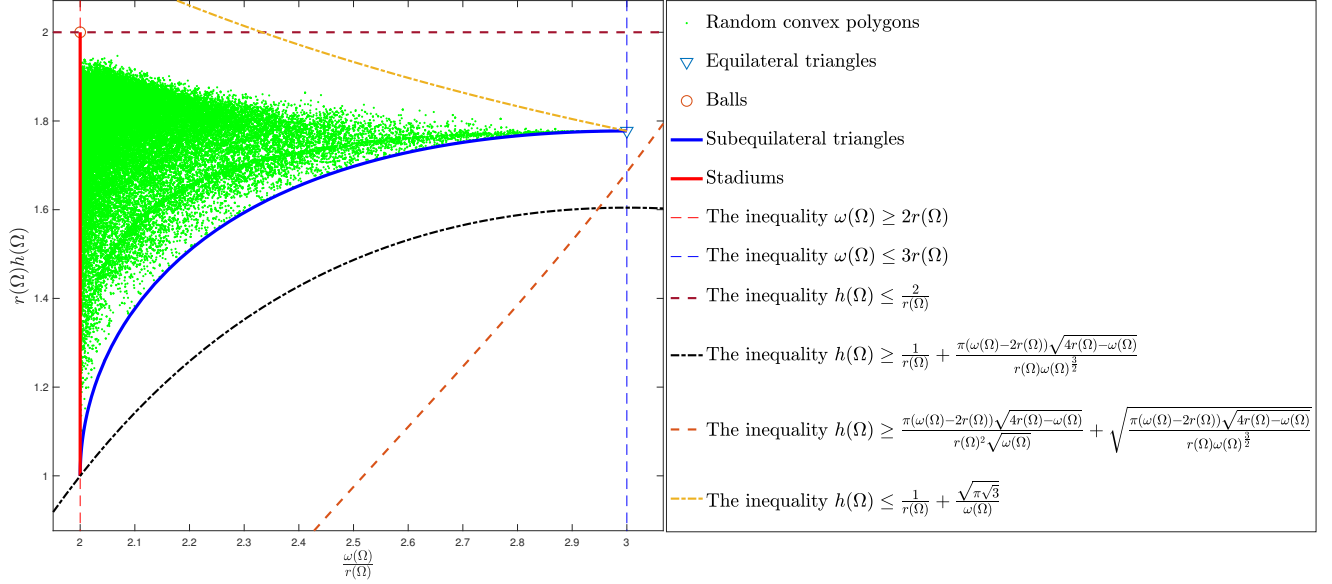
which ends the proof. \square

Remark 5.10. *It is possible to prove the following upper bound*

$$h(\Omega) \leq \frac{1}{r(\Omega)} + \frac{\sqrt{\pi\sqrt{3}}}{\omega(\Omega)},$$

where the equality holds for equilateral triangles, see Figure 17.

In order to prove it, one may combine the upper bound in (2) and the inequality $\omega(\Omega)^2 \leq \sqrt{3}|\Omega|$, see [38].

FIGURE 17. Blaschke-Santaló diagram of the triplet (ω, h, r) .

6. CONCLUSIONS AND CONJECTURES

In this Section, we collect the conjectures that we deduced from the numerical approximation of the Blaschke-Santaló diagrams that we have plotted in the previous sections.

Conjecture 1. We consider the diagram (ω, h, d) plotted in Figure 10. Let $\Omega \in \mathcal{K}^2$, we conjecture that if $\frac{\sqrt{3}}{2}d(\Omega) \leq \omega(\Omega) \leq d(\Omega)$, then

$$h(\Omega) \leq h(Y)$$

where Y is a Yamanouti set (see Definition 2.15) such that $\omega(Y) = \omega(\Omega)$ and $d(Y) = d(\Omega)$.

Conjecture 2. We consider the diagram (ω, h, P) plotted in Figure 15. Let $\Omega \in \mathcal{K}^2$, we conjecture that, if $\pi\omega(\Omega) \leq P(\Omega) \leq 2\sqrt{3}\omega(\Omega)$, then

$$h(\Omega) \leq h(Y),$$

where Y is a Yamanouti set (see Definition 2.15) such that $P(Y) = P(\Omega)$ and $\omega(Y) = \omega(\Omega)$.

Conjecture 3. We consider the diagram (R, h, d) plotted in Figure 16. Let $\Omega \in \mathcal{K}^2$, we conjecture that

$$h(\Omega) \geq h(N),$$

where N refers to a nonagon of constant width such that $d(N) = d(\Omega)$ and $R(N) = R(\Omega)$ described in [22] as follows: let Γ and γ be the circumcircle and the incircle of a constant width set K that are known to be concentric and such that $d(K) = \omega(K) = R(K) + r(K)$. The extremal set can be constructed in the following way: an equilateral triangle ABC is inscribed in the circle Γ , and now we take the circular arcs of radius $R(K) + r(K)$ drawn about the three vertex points. These arcs touch γ at the opposite points $\bar{A}, \bar{B}, \bar{C}$ of A, B, C , respectively. Furthermore, we construct three circles of radius $(R(K) + r(K))/2$ that have the sides of the triangle as chords and whose centers lie inside the triangle. The required constant width set has 3-fold symmetry and is formed by nine arcs of the six constructed circles, see Figure 18.

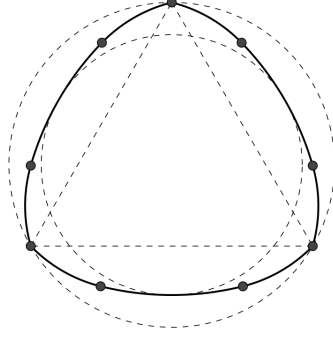


FIGURE 18. A nonagon of constant width.

Conjecture 4. We consider the diagram (ω, h, R) plotted in Figure 12. Let $\Omega \in \mathcal{K}^2$, we conjecture that:

- If $\omega(\Omega) \in [\frac{3}{2}R(\Omega), \sqrt{3}R(\Omega)]$, then

$$h(\Omega) \leq h(Y),$$

where Y is a Yamanouti set (see Definition 2.15) such that $\omega(Y) = \omega(\Omega)$ and $R(Y) = R(\Omega)$.

- If $\omega(\Omega) \geq \sqrt{3}R(\Omega)$, then

$$h(\Omega) \leq h(N),$$

where N refers to a nonagon of constant width such that $\omega(N) = \omega(\Omega)$ and $R(N) = R(\Omega)$.

7. APPENDIX: SUMMARY TABLES WITH THE RESULTS

In this first table, we summarize the results relative to the diagrams that are completely solved.

Param.	Condition	Inequality	Extremal sets	Ref.
P, h, A		$h \leq \frac{P}{A}$ $h \geq \frac{P + \sqrt{4\pi A}}{2A}$	Cheeger of itself sets that are homothetic to their form bodies	[16] [16]
r, h, A		$h \leq \frac{1}{r} + \sqrt{\frac{\pi}{A}}$ $h \geq \frac{1}{r} + \frac{\pi r}{A}$	sets that are homothetic to their form bodies stadiums	[14] [14]
P, h, r		$h \leq \frac{1}{r} + \sqrt{\frac{2\pi}{Pr}}$ $h \geq \frac{1}{r} + \frac{\pi}{P - \pi r}$	sets that are homothetic to their form bodies stadiums	Prop. 4.1 Prop. 4.1
d, h, r		$h \leq \frac{1}{r} + \sqrt{\frac{\pi}{r\sqrt{d^2 - 4r^2} + r^2(\pi - 2\arccos(\frac{2r}{d}))}}$ $h \geq \frac{1}{t_{g_1^\Omega}} \text{ (i)}$ $h > \frac{4 - \pi}{d + 2r - \sqrt{(d + 2r)^2 - 2(4 - \pi)dr}}$	two-cup bodies spherical slices/smoothed nonagons thinning rectangles	Prop. 4.2 Prop. 4.2 Remark 4.4
R, h, r		$h \leq \frac{1}{r} + \sqrt{\frac{\pi}{2r(\sqrt{R^2 - r^2} + r\arcsin(\frac{r}{R}))}}$ $h \geq \frac{1}{t_{g_2^\Omega}} \text{ (ii)}$ $h > \frac{4 - \pi}{2(R + r) - \sqrt{4(R + r)^2 - 4(4 - \pi)Rr}}$	two-cup bodies spherical slices thinning rectangles	Prop. 4.5 Prop. 4.5 Remark 4.6

(i) $t_{g_1^\Omega}$ is the smallest solution on $[0, r(\Omega)]$ to

$$g_1^\Omega(t) := \psi(d(\Omega) - 2t, r(\Omega) - t) = \pi t^2,$$

where

$$\psi(d, r) := \begin{cases} \frac{3\sqrt{3}r}{2}(\sqrt{d^2 - 3r^2} - r) + \frac{3d^2}{2}\left(\frac{\pi}{3} - \arccos\left(\frac{\sqrt{3}r}{d}\right)\right), & \text{if } d \leq rD^* \\ r\sqrt{d^2 - 4r^2} + \frac{d^2}{2}\arcsin\left(\frac{2r}{d}\right), & \text{if } d \geq rD^*. \end{cases}$$

and D^* is the unique number in $[2, 2\sqrt{3}]$ for which the two expression of the function $\psi(d, r)$ are equal.

(ii) $t_{g_2^\Omega}$ is the smallest solution on $[0, r(\Omega)]$ to

$$g_2^\Omega(t) := 2\left((r - t)\sqrt{(R(\Omega) - t)^2 - (r(\Omega) - t)^2} + (R(\Omega) - t)^2 \arcsin\left(\frac{r(\Omega) - t}{R(\Omega) - t}\right)\right) = \pi t^2.$$

In this second table, we summarize the results of the partially solved Blaschke–Santaló diagrams.

Param.	Condition	Inequality	Extremal sets	Ref.
ω, h, d	$\omega \leq \sqrt{3}/2d$	$h \leq \frac{1}{r(\omega, d)} + \sqrt{\frac{2\pi}{\omega d}} \text{ (iii)}$	subequilateral triangles	Prop. 5.1
	$\sqrt{3}/2d \leq \omega \leq d$	$h \leq \frac{\sqrt{3}}{\sqrt{3}\omega - d} + \sqrt{\frac{2\pi}{\pi\omega^2 - \sqrt{3}d^2 + 6\omega(\tan(\arccos(\frac{\omega}{d})) - \arccos(\frac{\omega}{d}))}}$	equilateral triangles	
		$h \geq \frac{1}{t_{g_3^\Omega}} \text{ (iv)}$	spherical slices	
		$h > \frac{1}{\omega} + \frac{1}{d} + \sqrt{\left(\frac{1}{\omega} + \frac{1}{d}\right)^2 - \frac{4-\pi}{\omega d}}$	thinning rectangles	Remark 5.2
ω, h, R	$\omega \leq 3/2R$	$h \leq \frac{1}{r(\omega, R)} + \sqrt{\frac{\pi}{A(\omega, R)}} \text{ (v)}$	subequilateral triangles	Prop. 5.3
		$h \geq \frac{1}{t_{g_4^\Omega}} \text{ (vi)}$	spherical slices	Remark 5.4
		$h \geq \frac{4-\pi}{(2R+\omega) - \sqrt{(2R+\omega)^2 - 2(4-\pi)R\omega}}$	thinning rectangles	
ω, h, P	$P \geq 2\sqrt{3}\omega$	$h \leq \frac{1}{r(\omega, P)} + \sqrt{\frac{\pi}{A(\omega, P)}} \text{ (vii)}$ $h \geq \frac{2}{\omega} + \frac{2\pi}{2P - \pi\omega}$	subequilateral triangles stadiums	Prop. 5.7
ω, h, A		$h \leq \frac{1}{r(\omega, A)} + \sqrt{\frac{\pi}{A}} \text{ (viii)}$ $h \geq \frac{2}{\omega} + \frac{\pi\omega}{2A}$	subequilateral triangles stadiums	Prop. 5.5
R, h, d		$h \leq \frac{2R(2R + \sqrt{4R^2 - d^2})}{d^2\sqrt{4R^2 - d^2}} + \sqrt{\frac{4\pi R^2}{d^3\sqrt{4R^2 - d^2}}}$	subequilateral triangles	Prop. 5.8
ω, h, r		$h \geq \frac{1}{r} + \frac{1}{r}\sqrt{\pi\left(1 - \frac{2r}{\omega}\right)\sqrt{\frac{4r}{\omega} - 1}}$	subequilateral triangles	Prop. 5.9

(iii) $r(\omega, d)$ is given by

$$d^2 (\omega - 2r(\omega, d))^2 (4r(\omega, d) - \omega) = 4r^4(\omega, d) \omega.$$

(iv) $t_{g_3^\Omega}$ is the smallest solution to

$$g_3^\Omega(t) := f(d(\Omega) - 2t, \omega(\Omega) - 2t) = \pi t^2,$$

where

$$f(d, w) = \frac{w}{2}\sqrt{d^2 - w^2} + \frac{d^2}{2}\arcsin\left(\frac{w}{d}\right)$$

(v) $r(\omega, R)$ is given by

$$(4r(\omega, R) - \omega) (\omega - 2r(\omega, R)) = \frac{2r^3(\omega, R)}{R}$$

and $A(\omega, R)$ is given by

$$16A(\omega, R)^6 = R^2\omega^2 (16A(\omega, R)^4 - R^2\omega^6).$$

(vi) $t_{g_4^\Omega}$ is the smallest solution on $[0, r(\Omega)]$ to

$$g_4^\Omega(t) := \chi(\omega(\Omega) - 2t, R(\Omega) - t) = \pi t^2,$$

where

$$\chi(\omega, R) := \frac{\omega}{2} \sqrt{4R^2 - \omega^2} + 2R^2 \arcsin \frac{\omega}{2R}.$$

(vii) $r(\omega, P)$ is given by

$$(\omega - 2r(\omega, P))^2(4r(\omega, P) - \omega)P^2 = 4r(\omega, P)^2\omega^3$$

and $A(\omega, P)$ is the middle root of the equation

$$128PA(\omega, P)^3 - 16\omega(5P^2 + \omega^2)A(\omega, P)^2 + 16\omega^2P^3A(\omega, P) - \omega^3P^4 = 0$$

(viii) $r(\omega, A)$ is given by

$$(\omega - 2r(\omega, A))^2(4r(\omega, A) - \omega)A^2 = r^4(\omega, A)\omega^3.$$

Finally, in this last table, we have summarized the inequalities that we have found and that do not correspond to parts of the boundaries of the corresponding Blaschke–Santaló diagrams.

Param.	Condition	Inequality	Extremal sets	Ref.
R, h, A		$h < \frac{1}{R} + \frac{4R}{A}$ $h \geq \frac{1}{2R} + \frac{\pi R}{2A} + \sqrt{\frac{\pi}{A}}$	thinning rectangles balls	[16, 38]
P, h, R		$h < \frac{P}{R(P-4R)}$ $h \geq \frac{4 \operatorname{arcsinc}\left(\frac{4R}{P}\right)}{P-4R \cos\left(\operatorname{arcsinc}\left(\frac{4R}{P}\right)\right)} + \sqrt{\frac{8\pi \operatorname{arcsinc}\left(\frac{4R}{P}\right)}{P(P-4R \cos\left(\operatorname{arcsinc}\left(\frac{4R}{P}\right)\right))}} \quad (ix)$	thinning rectangles balls	[16, 36]
P, h, d	$2d < P < 3d$ $3d \leq P \leq \pi d$	$h < \frac{4}{P-2d} + \sqrt{\frac{4\pi}{(P-2d)\sqrt{P(4d-P)}}}$ $h < \frac{4}{P-2d} + \sqrt{\frac{4\pi}{\sqrt{3}d(P-2d)}}$ $h \geq \frac{4 \operatorname{arcsinc}\left(\frac{2d}{P}\right)}{P-2d \cos\left(\operatorname{arcsinc}\left(\frac{2d}{P}\right)\right)} + \sqrt{\frac{8\pi \operatorname{arcsinc}\left(\frac{2d}{P}\right)}{(P-2d \cos\left(\operatorname{arcsinc}\left(\frac{2d}{P}\right)\right))}} \quad (ix)$	balls	[14, 16, 38]
d, h, A		$h \leq \frac{4}{d} + \frac{2d}{A}$ $h < \frac{2d}{A} + \sqrt{\frac{\pi}{A}}$ $h > \frac{d}{A} + \sqrt{\frac{\pi}{A}}$	thinning two-cup	[14, 16, 38]

(ix) where the cardinal-arcsine is defined as

$$\operatorname{sinc} : x \in \mathbb{R} \mapsto \operatorname{sinc}(x) = \frac{\sin(x)}{x}, \quad \operatorname{arcsinc}(x) = \operatorname{sinc}^{-1}(x)$$

Acknowledgements: The author would also like to thank the anonymous referees for their careful reading and useful comments that helped to improve the manuscript.

The authors would also like to thank Jimmy Lamboley for useful discussions.

I. Ftouhi and G. Paoli are supported by the Alexander von Humboldt Foundation through Alexander von Humboldt grants for Postdocs.

A. L. Masiello and G. Paoli are partially supported by GNAMPA of INdAM.

REFERENCES

- [1] F. Alter and V. Caselles. Uniqueness of the Cheeger set of a convex body. *Nonlinear Anal.*, 70(1):32–44, 2009.
- [2] K. R. Anderson. A reevaluation of an efficient algorithm for determining the convex hull of a finite planar set. *Inform. Process. Lett.*, 7(1):53–55, 1978.
- [3] P. R. S. Antunes and A. Henrot. On the range of the first two Dirichlet and Neumann eigenvalues of the Laplacian. *Proc. R. Soc. Lond. Ser. A Math. Phys. Eng. Sci.*, 467(2130):1577–1603, 2011.

- [4] B. Appleton and H. Talbot. Globally minimal surfaces by continuous maximal flows. *IEEE Transactions on Pattern Analysis and Machine Intelligence*, 28(1):106–118, 2006.
- [5] W. Blaschke. Eine frage über konvexe Körper. *Jahresber. Deutsch. Math. Ver.*, 25:121–125, 1916.
- [6] B. Bogosel, D. Bucur, and I. Fragalà. Phase field approach to optimal packing problems and related Cheeger clusters. *Appl. Math. Optim.*, 81(1):63–87, 2020.
- [7] B. Bogosel, G. Buttazzo, and E. Oudet. On the numerical approximation of blaschke-santaló diagrams using centroidal voronoi tessellations, 2023.
- [8] T. Bonnesen and W. Fenchel. *Theory of convex bodies*. BCS Associates, Moscow, ID, 1987. Translated from the German and edited by L. Boron, C. Christenson and B. Smith.
- [9] K. Böröczky, Jr., M. A. Hernández Cifre, and G. Salinas. Optimizing area and perimeter of convex sets for fixed circumradius and inradius. *Monatsh. Math.*, 138(2):95–110, 2003.
- [10] R. Brandenburg and B. González Merino. A complete 3-dimensional Blaschke-Santaló diagram. *Math. Inequal. Appl.*, 20(2):301–348, 2017.
- [11] R. Brandenburg and B. G. Merino. On (r, d, R) -Blaschke-Santaló diagrams with regular k -gon gauges. *to appear in Revista de la Real Academia de Ciencias Exactas, Físicas y Naturales. Serie A, Matemáticas*, 2022.
- [12] J. Cheeger. A lower bound for the smallest eigenvalue of the Laplacian. *A Symposium in Honor of Salomon Bochner*, page 195–199, 1970.
- [13] A. Delyon, A. Henrot, and Y. Privat. The missing (A, D, r) diagram. *Ann. Inst. Fourier (Grenoble)*, 72(5):1941–1992, 2022.
- [14] I. Ftouhi. On the Cheeger inequality for convex sets. *J. Math. Anal. Appl.*, 504(2):Paper No. 125443, 26, 2021.
- [15] I. Ftouhi. Optimal description of Blaschke-Santaló diagrams via numerical shape optimization. <https://hal.archives-ouvertes.fr/hal-03646758>, 2022. preprint.
- [16] I. Ftouhi. Complete systems of inequalities relating the perimeter, the area and the Cheeger constant of planar domains. *Communications in Contemporary Mathematics*, 25(10), 2023.
- [17] I. Ftouhi and A. Henrot. The diagram (λ_1, μ_1) . *Math. Rep. (Bucur.)*, 24(74)(1-2):159–177, 2022.
- [18] I. Ftouhi and J. Lamboley. Blaschke-Santaló diagram for volume, perimeter, and first Dirichlet eigenvalue. *SIAM J. Math. Anal.*, 53(2):1670–1710, 2021.
- [19] M. Henk and G. A. Tsintsifas. Some inequalities for planar convex figures. *Elem. Math.*, 49(3):120–125, 1994.
- [20] A. Henrot and M. Pierre. *Shape variation and optimization*, volume 28 of *EMS Tracts in Mathematics*. European Mathematical Society (EMS), Zürich, 2018.
- [21] M. A. Hernández Cifre. Is there a planar convex set with given width, diameter, and inradius? *Amer. Math. Monthly*, 107(10):893–900, 2000.
- [22] M. A. Hernández Cifre. Optimizing the perimeter and the area of convex sets with fixed diameter and circumradius. *Arch. Math. (Basel)*, 79(2):147–157, 2002.
- [23] M. A. Hernández Cifre and S. Gomis. The missing boundaries of the Santaló diagrams for the cases (d, ω, R) and (ω, R, r) . *Discrete Comput. Geom.*, 23(3):381–388, 2000.
- [24] M. A. Hernández Cifre and G. Salinas. Some optimization problems for planar convex figures. Number 70, part I, pages 395–405. 2002. IV International Conference in “Stochastic Geometry, Convex Bodies, Empirical Measures & Applications to Engineering Science”, Vol. I (Tropea, 2001).
- [25] M. A. Hernández Cifre, G. Salinas, and S. Gomis. Complete systems of inequalities. *Journal of inequalities in pure and applied mathematics*, 2(1), March 2001.
- [26] T. Jahn. Extremal radii, diameter and minimum width in generalized Minkowski spaces. *Rocky Mountain J. Math.*, 47(3):825–848, 2017.
- [27] B. Kawohl and T. Lachand-Robert. Characterization of Cheeger sets for convex subsets of the plane. *Pacific J. Math.*, 225(1):103–118, 2006.
- [28] J. B. Keller. Plate failure under pressure. *SIAM Review*, 22(11):227–228, 1980.
- [29] T. Kubota. Einige ungleichheitsbeziehungen über eilinien und eiflächen. *Sci. Rep. of the Tohoku Univ. Ser. (1)*, 12:45–65, 1923.
- [30] S. Larson. Corrigendum to “A bound for the perimeter of inner parallel bodies” [J. Funct. Anal. 271 (3) (2016) 610–619]. *J. Funct. Anal.*, 279(5):108574, 2, 2020.
- [31] I. Lucardesi and D. Zucco. On Blaschke-Santaló diagrams for the torsional rigidity and the first Dirichlet eigenvalue. *Ann. Mat. Pura Appl. (4)*, 201(1):175–201, 2022.
- [32] E. Parini. An introduction to the Cheeger problem. *Surv. Math. Appl.*, 6:9–21, 2011.
- [33] E. Parini. Reverse Cheeger inequality for planar convex sets. *J. Convex Anal.*, 24(1):107–122, 2017.
- [34] F. P. Preparata and M. I. Shamos. *Computational geometry*. Texts and Monographs in Computer Science. Springer-Verlag, New York, 1985. An introduction.
- [35] V. Sander. <https://cglab.ca/~sander/misc/ConvexGeneration/convex.html> [Accessed: 31/01/2024].

- [36] L. Santaló. Sobre los sistemas completos de desigualdades entre treselementos de una figura convexa plana. *Math. Notae*, 17:82–104, 1961.
- [37] R. Schneider. *Convex Bodies: The Brunn-Minkowski Theory*. Cambridge University Press, 2nd expanded edition edition, 2013.
- [38] P. R. Scott and P. W. Awyong. Inequalities for convex sets. *JIPAM. J. Inequal. Pure Appl. Math.*, 1(1):Article 6, 6, 2000.
- [39] M. Sholander. On certain minimum problems in the theory of convex curves. *Trans. Amer. Math. Soc.*, 73:139–173, 1952.
- [40] G. Strang. Maximal flow through a domain. *Math. Programming*, 26(2):123–143, 1983.
- [41] P. Valtr. Probability that n random points are in convex position. *Discrete Comput. Geom.*, 13(3-4):637–643, 1995.
- [42] M. van den Berg, G. Buttazzo, and A. Pratelli. On relations between principal eigenvalue and torsional rigidity. *Commun. Contemp. Math.*, 23(8):Paper No. 2050093, 28, 2021.
- [43] M. Yamanouti. Notes on closed convex figures. *Proc. Phys.-Math. Soc. Japan, III. Ser.*, 14:605–609, 1932.

(Ilias Ftouhi) FRIEDRICH-ALEXANDER-UNIVERSITÄT ERLANGEN-NÜRNBERG, DEPARTMENT OF MATHEMATICS, CHAIR OF APPLIED ANALYSIS (ALEXANDER VON HUMBOLDT PROFESSORSHIP), CAUERSTR. 11, 91058 ERLANGEN, GERMANY.
Email address: `ilias.ftouhi@fau.de`

(Alba Lia Masiello (Corresponding Author)) DIPARTIMENTO DI MATEMATICA E APPLICAZIONI "R. CACCIOPPOLI", UNIVERSITÀ DEGLI STUDI DI NAPOLI "FEDERICO II", COMPLESSO UNIVERSITARIO MONTE S. ANGELO, VIA CINTIA - 80126 NAPOLI, ITALY.
Email address: `albalia.masiello@unina.it`

(Gloria Paoli) DIPARTIMENTO DI MATEMATICA E APPLICAZIONI "R. CACCIOPPOLI", UNIVERSITÀ DEGLI STUDI DI NAPOLI "FEDERICO II", COMPLESSO UNIVERSITARIO MONTE S. ANGELO, VIA CINTIA - 80126 NAPOLI, ITALY.
Email address: `gloria.paoli@unina.it`